Neural Networks 37 (2013) 66–92

Contents lists available at SciVerse ScienceDirect

Neural Networks

journal homepage: www.elsevier.com/locate/neunet

Synthetic event-related potentials: A computational bridge between neurolinguistic models and experiments

Victor Barrès [a,b], Arthur Simons III [b], Michael Arbib [a,b,c,*]

[a] Neuroscience Graduate Program, University of Southern California Los Angeles, CA 90089-2520, USA
[b] USC Brain Project, University of Southern California Los Angeles, CA 90089-2520, USA
[c] Computer Science Department, University of Southern California Los Angeles, CA 90089-2520, USA

ARTICLE INFO

Keywords:
Event-related potential
Forward model
Neurolinguistics
Schema theory
Neural network
Computational model
Conceptual model
Synthetic Brain Imaging
EEG
Language

ABSTRACT

Our previous work developed Synthetic Brain Imaging to link neural and schema network models of cognition and behavior to PET and fMRI studies of brain function. We here extend this approach to Synthetic Event-Related Potentials (Synthetic ERP). Although the method is of general applicability, we focus on ERP correlates of language processing in the human brain. The method has two components: Phase 1: To generate cortical electro-magnetic source activity from neural or schema network models; and Phase 2: To generate known neurolinguistic ERP data (ERP scalp voltage topographies and waveforms) from putative cortical source distributions and activities within a realistic anatomical model of the human brain and head. To illustrate the challenges of Phase 2 of the methodology, spatiotemporal information from Friederici's 2002 model of auditory language comprehension was used to define cortical regions and time courses of activation for implementation within a forward model of ERP data. The cortical regions from the 2002 model were modeled using atlas-based masks overlaid on the MNI high definition single subject cortical mesh. The electromagnetic contribution of each region was modeled using current dipoles whose position and orientation were constrained by the cortical geometry. In linking neural network computation via EEG forward modeling to empirical results in neurolinguistics, we emphasize the need for neural network models to link their architecture to geometrically sound models of the cortical surface, and the need for conceptual models to refine and adopt brain-atlas based approaches to allow precise brain anchoring of their modules. The detailed analysis of Phase 2 sets the stage for a brief introduction to Phase 1 of the program, including the case for a schema-theoretic approach to language production and perception presented in detail elsewhere. Unlike Dynamic Causal Modeling (DCM) and Bojak's mean field model, Synthetic ERP builds on models of networks that mediate the relation between the brain's inputs, outputs, and internal states in executing a specific task. The neural networks used for Synthetic ERP must include neuroanatomically realistic placement and orientation of the cortical pyramidal neurons. These constraints pose exciting challenges for future work in neural network modeling that is applicable to systems and cognitive neuroscience.

1. Background

In the present section, we briefly look at the advantages and drawbacks of fMRI and synthetic brain imaging and then briefly review the use of Event-Related Potential (ERP) data in neurolinguistics. To complete the background, we briefly describe how inverse and forward models relate ERPs to electrical signals within the brain.

1.1. fMRI and Synthetic Brain Imaging

We have previously explored how simulations of neural networks constrained by data from animal neurophysiology can emulate adaptive and visuomotor behavior (e.g. Fagg & Arbib, 1992; Schweighofer, Arbib, & Dominey, 1996). With the advent of tomographic brain imaging, the lab expanded this simulation method to develop Synthetic Brain Imaging. Synthetic PET (Arbib, Bischoff, Fagg, & Grafton, 1995) facilitated modeling and comparison of saccade generation in primates and humans, and a similar approach was used to associate a synthetic BOLD signal with a model of primate imitation (Arbib, Billard, Iacoboni, and Oztop (2000), see Husain, Tagamets, Fromm, Braun, and Horwitz (2004), Tagamets and Horwitz (1998) for related studies). The key idea is to start with a biologically grounded neural network

* Correspondence to: Computer Science, Neuroscience and the USC Brain Project, University of Southern California, Los Angeles, CA 90089-2520, USA. Tel.: +1 213 740 9220; fax: +1 213 821 3046.
E-mail addresses: barres@usc.edu (V. Barrès), arthursimons3@gmail.com (A. Simons III), arbib@usc.edu (M. Arbib).

0893-6080/$ – see front matter © 2012 Elsevier Ltd. All rights reserved.
doi:10.1016/j.neunet.2012.09.021

for executing a task set that matches a range of neurophysiological and behavioral data. A spatial and temporal average over the simulated absolute value of all synaptic activations across a region provides a viable prediction of the activation of that region for brain imaging — thus enabling the use of simulations of biologically grounded neural networks to yield predictions to be tested against brain imaging studies. Here we initiate a comparable methodology for Synthetic ERP to allow us to provide a bridge between computational models of fine-grained processes in the brain and ERP data. We focus on computational models that *simulate the information processing required to perform a given task*. As we show in Section 1.3, this emphasis distinguishes the new method from Dynamic Causal Modeling (DCM) and Bojak's mean field model although certain techniques are common to the three methods. We concentrate our work on neural network models but we also discuss schema level computational models. Although the method should have broad applicability the focus of this paper is on ERP data related to language processing.

To set the stage we briefly compare three sources of data for neurolinguistics: lesions, fMRI (or PET), and ERPs. There has historically been a disconnect between processing models of neurolinguistics which seek to derive linguistic phenomena from empirical data and biological constraints (Kempen & Hoenkamp, 1987), and representational approaches which employ a top–down approach seeking to assign theories of language structure to biological systems (Lecours & Lhermitte, 1969). Computational modeling was advanced as a means to reconcile these methods (Arbib & Caplan, 1979), but because lesion data were the primary data linking brain and language at that time, the attempt to assign linguistic processing to specific cortical regions remained problematic. New techniques for lesion studies combined with subsequent hemodynamic imaging techniques allowed the researchers to support neurolinguistic models at the level of interacting brain regions (e.g. Hagoort, 2005; Hickok & Poeppel, 2007), but such models often give an all-or-none match of region to function inconsistent with the dynamics of neural interactions across the brain. Computational approaches like Synthetic Brain Imaging are needed to relate such interactions to hypotheses about detailed neural circuitry or schema interactions. To extend Synthetic Brain Imaging to simulate higher cognitive functions such as language for which there are no animal data, one may explore homologies between the macaque and human brain as a basis for evolutionary hypotheses that suggest possible circuitry within areas of the human brain associated with uniquely human functions (Arbib & Bota, 2003).

1.2. Event-related potentials: A privileged window into how the brain processes language

Hemodynamic imaging techniques provide an indirect measurement of neuronal activity mediated by the mechanisms of perfusion and metabolism, resulting in a physiological limit in their temporal resolution on the order of seconds (Heeger & Ress, 2002). Unlike PET or fMRI, recordings of neuroelectromagnetic activity taken by electroencephalography (EEG) and Magnetoencephalography (MEG) are reputed to allow one to follow the time course of neural activity on a time scale of milliseconds rather than seconds — but at the high price of a drastic loss of spatial resolution. Neuroelectromagnetic fields are thought to originate within the apical dendrites of cortical pyramidal neuron populations synchronously engaged in excitatory depolarizations and inhibitory hyperpolarizations in postsynaptic potentials (EPSPs and IPSPs respectively) (Niedermeyer & Silva, 2010). Unlike the radial symmetry exhibited by their basal dendrites, the linear orientation of the pyramidal cell's apical dendrites provides the basis for generation of a net dipole moment during EPSPs and IPSPs (Ritter, Vaughan, & Simson, 1983). The polarized geometry of the pyramidal cell's apical dendrites is repeated at the population level through the organization of pyramidal cells into a palisade formation where the axes of the cells' dendritic trees parallel one another perpendicularly to the cortical surface (Nunez & Silberstein, 2000, and see also Appendix B). The rationale for viewing EPSPs and IPSPs rather than action potentials as the electrophysiological phenomenon underpinning EEG-recorded scalp potentials is based on the recognition that only synchronous (de)polarizations of neural populations would be able to produce measurable signals at the scalp. While action potentials have a significantly larger amplitude (100 mV vs. 10 mV), the PSP's time course is longer in duration (10 ms vs. 1 ms) and thereby allows more opportunity for synchronization. Such electrical summation plus relative proximity to the scalp satisfies the theoretical conditions for the activity of cortical pyramidal neurons to generate the electromagnetic fields perceived on the scalp surface (Lopes da Silva & Van Rotterdam, 1987).

An encephalogram is obtained by recording an array of potentials from leads attached at various places on the scalp (i.e., external to the head) over a certain time period. ERPs are extracted from the encephalogram by averaging recordings of signals at each lead over a number of trials using the same task and with recordings time-locked to stimulus onset. The challenge for interpretation of the ERP is to correctly divide the average waveform into various components that may be viewed as measurements of distinct cognitive processes relevant to the task at hand. When researchers cite the presence of a given ERP component in response to an experimental stimulus (dotted line in Fig. 1), they are generally referring to a statistically significant increase in the component's intensity compared to its baseline intensity observed with a control stimulus (solid line in Fig. 1).

From 1980 onwards, ERPs have supplied an important method of investigation for neurolinguistic research (see Fig. 1 for examples in German). The first significant contribution came with the discovery of an increased negativity (shown as an upward deflection in ERP displays!), the N400 event-related potential, which occurs approximately 400 ms after the start of presentation of a *semantically* anomalous word within a sentence (Kutas & Hillyard, 1980), suggesting that the N400 may signal "reprocessing" of semantically anomalous information. (Osterhout & Holcomb, 1992) saw an increased positive brain potential 600 ms (P600) after the onset of words which were syntactically inconsistent with the preceding words of the sentence. Furthermore, final words in sentences typically judged to be unacceptable elicited an N400-like effect, relative to final words in sentences typically judged to be acceptable. In this way, ERPs offer precise timing data, but the distribution of potentials across the scalp does not support a confident inference of where in the brain these changes are elicited (more on this when we discuss Fig. 4). A number of neurolinguistic models thus seek to integrate the functional localization from tomographic imaging with the functional time course from ERP recordings and thereby arrive at a spatiotemporal account of various functional components of language processing. However, such an account does not address the issues of what information is represented in diverse brain regions and how they interact with each other in language processing. As we shall later spell out in detail, this gap motivates our initial work on Synthetic ERPs presented here, seeking to relate ERPs to detailed processing models.

1.3. Synthetic ERP in comparison to dynamic causal modeling and other ERP modeling approaches

Perhaps the ERP modeling approach with most in common with Synthetic ERP is Dynamic Causal Modeling (DCM). The focus of this section, then, is to not only chart those commonalities but also

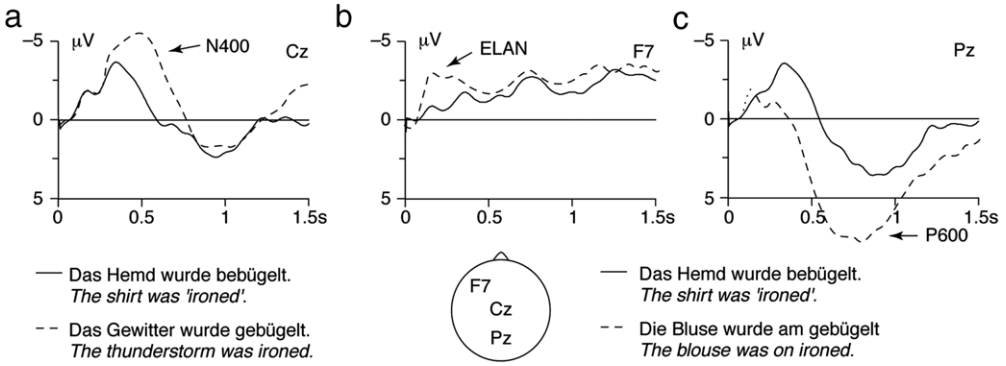

Fig. 1. Three language-related components in the ERP: (a) the semantic N400, (b) the syntactic early left-anterior negativity (ELAN), and (c) P600. Solid lines represent the condition for a correct word, and dotted lines the condition for an anomalous word.
Source: Adapted from Friederici (2002).

make explicit the ways in which our approach diverges from DCM. (In Table 1 we will offer an explicit comparison of Synthetic ERP not only with DCM but also with Bojak's mean field model.) To preview what follows, the difference turns on the word "causal". For DCM, the issue is "What aggregated measures of underlying neural activity could cause the observed ERP recordings?" whereas Synthetic ERP is *doubly* causal: "(1) What patterns of interaction in neural circuitry could cause the observed behavior (and, where available, explain single-cell recordings)?; and (2) Could the aggregate activity of neurons in the circuitry so modeled cause the observed ERP recordings?"

As previously mentioned, current models of neurolinguistic processing seek to integrate the temporal and spatial information obtained from electromagnetic recording and hemodynamic imaging respectively. To accomplish this integration, researchers have sought to model different ERP component's "neural generators" through the use of equivalent current dipoles whose location, orientation and amplitude are considered to approximate the synaptic activity of pyramidal cells in some region or patch of cortex (see Appendix B for a more thorough presentation of the current dipole model). The attempt to infer generators from the scalp distribution of ERPs, commonly called the *inverse problem*, has long been recognized as an ill-posed problem (Helmholtz, 1853) since many different patterns of neural activity can in theory result in similar EEG recordings (Nunez & Srinivasan, 2005). Accordingly, the use of a priori constraints (which may be neurologically unrealistic) is required to generate a unique solution. Numerous approaches to the inverse problem have been developed including parametric approaches (Miltner, Braun, Johnson, Simpson, & Ruchkin, 1994), non-parametric approaches (Pascual-Marqui, Michel, & Lehmann, 1994), and constrained solution space approaches using PET or fMRI imaging (Bohland, Bullock, & Guenther, 2009; Phillips, Rugg, & Friston, 2002), and much energy has been spent comparing their various merits and the situation-dependent applicability of their respective a priori constraints (Grech, Cassar, Muscat, Camilleri, & Fabri, 2008; Michel et al., 2004). However, the *forward problem* of going from a set of dipoles via a representation of brain/skull/scalp geometries and conductivities to yield scalp potentials is well-posed (though, as we shall see later, representing brain/skull/scalp geometries is a major challenge).

Our goal for Synthetic ERP consists in developing computational tools to link biological neural network models of brain functions to quantitative predictions of the EEG recordings generated by the neural activity in such models. The "biological" neural network approach differs from the "artificial" neural networks approach by its insistence that models should be constrained by biological data including: accurate characterization of discrete cell types, anchoring of sub-networks within specific brain regions, and connectivity structures reflecting the known connectivity of the brain. In addition, such models should be causally complete information processing models. By this we mean that the purpose of the models should be to simulate the behaviors of the organism performing a given motor, sensory, or cognitive task. This distinguishes Synthetic ERP from approaches which simulate neural masses solely in terms of fitting ERP data rather than modeling networks that mediate the relation between the brain's inputs, outputs, and internal states in executing a specific task. For example, the behavior of tens of thousands of neighboring neurons (neural masses) might be modeled by a few time varying mesoscopic parameters. So called neural mass or mean field models have been especially important in the field of EEG signal modeling with a focus on replicating epileptic seizures as well as the richness of known electrocortical rhythms. A comprehensive review of such models can be found in Deco, Jirsa, Robinson, Breakspear, and Friston (2008).

Table 1 presents a comparison of two EEG signal forward models with our Synthetic ERP approach. DCM and Bojak's mean field model were chosen because they represent two different modeling approaches which share a common goal with Synthetic ERP: to develop biologically realistic forward models. They differ in that DCM focuses on the inverse problem while Bojak et al. focus on the anatomical details of the forward model. We note that Sotero, Trujillo-Barreto, Iturria-Medina, Carbonell, and Jimenez (2007) developed an approach very similar to that of Bojak. The models are compared based on 4 types of characteristics: their computational approach, their use of anatomical constraints, the way the hypotheses represented by the models are linked to empirical evidence, and finally their suitability as inverse models for EEG neuroimaging source localization.

In terms of *computational approaches*, both DCM and Bojak's model use a network of mesoscopic neural masses (David & Friston, 2003; Jansen & Rit, 1995) or mean field models (Liley, Cadusch, & Dafilis, 2002) whose purpose is to account for large scale neural dynamics. The connections between neural masses reflect large-scale white matter connectivity but also, only in case of Bojak et al., local connectivity between neighboring cortical patches. Synthetic ERP on the other hand proposes to link causally complete neural networks models designed with the purpose not to simulate large-scale activation patterns but instead to simulate the information processing required to perform a cognitive task. Both long and short scale neural connectivity constraints can be incorporated in such networks.

The three models vary in their use of *anatomical constraints*. DCM models tend to put less emphasis on cortical topology and head geometry. However this is less an intrinsic limitation of the approach than a consequence of their focus on the Bayesian framework for hypothesis testing (see below). In contrast, Bojak's

Table 1
Comparison of three computational approaches for EEG/ERP forward modeling. From left to right: Dynamic Causal Modeling (DCM) (David et al., 2005, 2006); the mean field model described by Bojak et al. (2010); and finally our own Synthetic ERP approach. The models are compared according to characteristics related to their computational approach, their use of anatomical constraints, their mode of hypothesis testing including whether monkey neurophysiology data can be used to build hypotheses, and finally their emphasis (or lack thereof) on inverse modeling.

Characteristics		Models		
		DCM	Bojak et al. (2010)	Synthetic ERP
Computational approach	**General goal**	Biologically sound forward model of ERP usable in a Bayesian inverse model framework	Biologically sound whole brain forward model of EEG patterns	Biologically sound synthetic read-out of ERP signals from brain anchored network models
	Modeling focus	Large scale neural dynamics	Large scale neural dynamics	Causally complete information processing model
	Implementation level	Neural mass	Mean field	Biological neural (or schema) networks
Anatomical constraints	**Current dipole modeling**	Few dipoles	Dipole distributions for the whole cortex	Dipole distributions for relevant brain regions
	Source waveform	Read-out from pyramidal cell neural mass activity	Read-out from pyramidal cell neural mass activity	Read-out from pyramidal cell synaptic activity
	Anatomical constraints on the dipole sources	Position only	Position and orientation based on anatomically sound cortical geometry	Position and orientation based on anatomically sound cortical geometry
	Link to brain atlases	Not discussed	Not discussed	Emphasizes the issue of variation in cortical surface parcellation ontologies
	Structural connectivity within a brain region	Brain regions are modeled by a single dipole	Realistic connectivity between distributed dipoles	Based on the connectivity of the neural net layer representing the region
	Structural connectivity between brain regions	Based on existing literature	Based by homology on the CoCoMac database for the macaque connectome	Based on existing literature
	Anatomical constraints on the conduction volumes	Spherical head model	Realistic head model	Realistic head model
Hypothesis testing	**Free parameters estimation**	Probability distributions through Bayesian inference	Single values	Single values
	Model comparison	Bayesian model comparison (accounts for model complexity)	Based on capacity to simulate empirical results	Based on capacity to simulate empirical results
	Incorporate monkey neurophysiology data	No	Connectivity only	Connectivity and single-unit recording
Neuroimaging use	**Suitable for inverse modeling**	Yes	No	No

model puts a heavy emphasis on anatomical constraints for sources and volume conductor modeling. Sources are defined as distributions of current dipoles constrained in position and orientation by the geometry of the cortex. In addition, it uses the CoCoMac database for the macaque connectome (Stephan et al., 2001) to generate, by homology, the patterns of connectivity between human brain regions. Finally, Synthetic ERP follows Bojak and insists on the role of cortical geometry in current source modeling. In contrast to Bojak's whole brain modeling approach, Synthetic ERP only models those cortical regions implemented in the underlying neural network model, and in doing so tackles often ignored quantitative issues regarding the role that cortical surface parcellation ontologies, brain atlases, idiosyncratic cortical variations, and neurohomologies (in the case of the comparison of human and non-human primate brain structures) should play in modeling EEG signals.

All three approaches use computational models to express *hypotheses*. Synthetic ERP and Bojak et al. simply focus on generating the simulated EEG data associated with a given model. Such simulations can then be compared to empirical ERP results that support or invalidate the hypotheses made by the modeler. Embedded within a Bayesian inference framework, DCM has been specifically developed to allow for an optimal use of empirical evidence, e.g. ERPs, to infer an inverse solution defined as a neural mass network model. David, Maess, Eckstein, and Friederici (2011) and Yvert, Perrone-Bertolotti, Baciu, and David (2012) applied DCM to ERPs resulting from various linguistic tasks (prosodic and syntactic violations, phoneme detection in pseudo-words, and semantic categorization). They were able to optimally assign the evidence provided by ERP measurements to highlight the role that the subcortical thalamic relay could play in language comprehension as well as the potential structure and change of effective connectivities in various language-related neural pathways. Our current aim is to link forward modeling to computational neural networks that can causally explain an observed behavior as opposed to computational models of neural dynamics. While this approach does not immediately lend itself to discussions of optimal hypothesis testing, it underscores the great potential for incorporating data from non-human primate neurophysiology within neurolinguistic computational models. The focus of Synthetic ERP on such models will also facilitate framing neurolinguistic modeling into an evolutionary perspective that makes full use of both human and non-human primate data.

Finally, only DCM has been designed specifically to be used as an inverse model for neuroimaging use. Working outside the inverse modeling framework relaxes many assumptions commonly made to constrain the ill-posed inverse problem such as the limitation in the number of current sources.

Our Synthetic ERP approach follows in Bojak et al.'s footsteps by insisting on the importance of cortical geometry, but then goes beyond Bojak et al. in assigning computational models of neural or schema networks to the various brain regions, and insists on linking such networks to a 3D model of the region suited for forward EEG modeling. Departing from the use of neural masses and looking into the possibility of linking neural networks to ERP data, the Synthetic ERP approach insists on the relevance, from an evolutionary perspective, of such models that have been exhaustively used to model processing in the monkey brain. In this paper our methodology sidesteps the ill-posedness of the inverse model by showing how computational models of linguistic processes may be linked to dipole distributions modeling the neural electric activity resulting from the simulation of such processes, and how these in turn may — via forward modeling — yield scalp distributions of ERPs that can be tested against neurolinguistic data. Unfortunately, our analysis will reveal that current neurolinguistic models are inadequate for such detailed

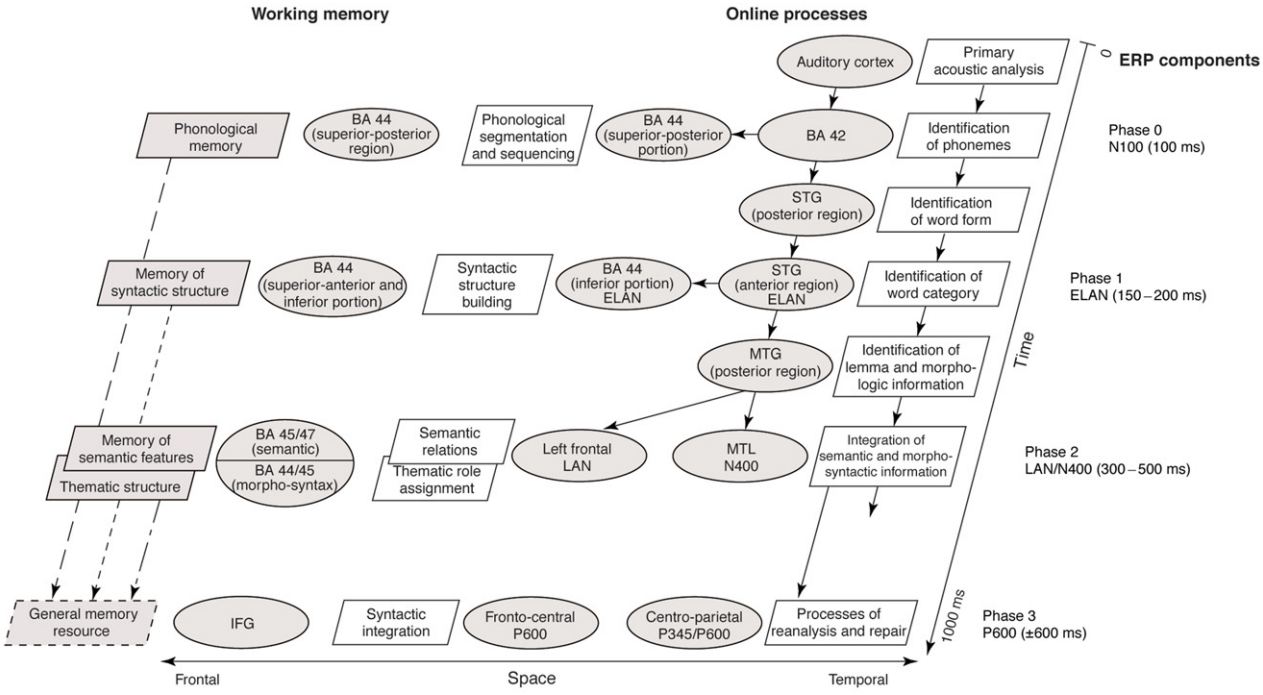

Fig. 2. A conceptual model of the time course and localization of activation of left hemisphere activity in response to hearing a word during the comprehension of a sentence. The right hand half will be referred to as "the 2002 model". The boxes represent the functional processes, the ellipses the underlying neural correlates. Abbreviations: BA, Brodmann's area; ELAN, early left-anterior negativity; IFG, inferior frontal gyrus; MTG, middle temporal gyrus; MTL, middle temporal lobe; PET, positron imaging tomography; STG, superior temporal gyrus.
Source: Adapted from Friederici (2002).

analysis, thus posing new challenges for both modeling and empirical studies.

2. "The 2002 model": Friederici's 2002 model of auditory sentence processing

2.1. A basic feedforward model of the timing and localization of processes involved in integrating the auditory form of a word into the comprehension of a sentence

Our aim in this paper is to introduce a new methodology, Synthetic ERP, and show its relevance to providing fine scale models (at the level of neural or schema networks) of brain processes underlying human use of language. To frame the issues involved and the challenges that our approach makes explicit for future research in neurolinguistics, we will focus on a conceptual model (as distinct from a processing model developed for computer simulation) of the temporal activation of brain areas during auditory sentence comprehension developed by Friederici (2002). Subsequent work has refined some aspects of this view (see Friederici, 2011, for her own update) and there are now many data from other laboratories that complicate the picture, but the 2002 model remains a valuable benchmark for the approach offered here. The key idea in forming the 2002 model was this: (a) Assess ERP data to time-stamp processes against the beginning of a word with certain characteristics relative to the preceding words of the sentence; and (b) seek other data (whether from PET, fMRI, TMS or lesion studies) that suggests the localization of the posited process. While some of the (a)–(b) matches are well-established, others remain debatable because we stress that (i) ERP data provides precise timing but offer little or no clue as to the source of an observed peak of potential; (ii) the non-ERP data may localize to the level of a general brain region but not to the level of specific circuits or subregions, and in any case cannot specify events with much less temporal precision than 1 s; (iii) different studies use different stimuli, making it unclear whether they elicit the same pattern of neural activity, and (iv) most of the time, multiple brain regions will be actively involved, though to varying degrees.

Fig. 2 shows the localization and timing of left hemisphere processes. The model posits four phases:

Phase 0 (0–100 ms): Acoustic analysis and phoneme identification correlate with the well-characterized auditory N100 ERP component.

Phase 1 (100–300 ms): The initial syntactic structure is formed on the basis of information about the word category. An Early Left-Anterior Negativity (ELAN) correlates with rapidly detectable word category errors.

Phase 2 (300–500 ms): Lexical-semantic and morphosyntactic processes support thematic role assignment (e.g., determining which noun phrase denotes the agent of the action described by the verb). A Left-Anterior Negativity (LAN) correlates with morphosyntactic errors. In this model, the N400 occurs in response to words that cannot be integrated semantically into the preceding context.

Phase 3 (500–1000 ms): The different types of information are integrated. A late centro-parietal positivity, the P600, occurs between 600–1000 ms and correlates with outright syntactic violations (following the ELAN) and with 'garden-path' sentences that require syntactic revision, and with processing of syntactically complex sentences.

On this view (see Friederici's Phase 1), linking a new word into a syntactic phrase structure is autonomous and precedes semantic analysis in the early-time windows; these processes interact only at later times. However, word-forms can be ambiguous as to syntactic category — e.g., *glass* can function as adjective or noun. Thus, semantic priming may dominate over syntactic category

in analyzing the word form; whereas in other cases multiple interpretations may be needed (at least transiently) to continue the parse, as in deciding how *glass* is being used in *the glass is half full* versus *the glass pendant is beautiful.* All this suggests possible refinements of the 2002 model, but these will not concern us explicitly in the present paper since our aim here is to establish a new methodology.

The model is conceptual rather than computational in that it does not describe the computations within each region, and does not assess what data must be "in play" from earlier words of the sentence (and the broader context) to affect how the current word is processed. Although the left hand sequence highlights memory processes and the processing of the current word at right is posited to update memory structures, the model shows only a forward flow from auditory input without showing how the working memory induced by earlier words of a sentence feeds back to affect the processing of the current word. In particular, there is no way for semantic features (Phase 2) to contribute to the initial updating of syntactic structure (Phase 1) — rather, it is only in Phase 3 that problems in syntactic analysis are claimed to trigger processes of reanalysis and repair that may invoke semantic features. Note how different aspects of each word are evoked in different regions during different phases — suggesting a distributed representation of the lexicon but one whose components are accessed in serial fashion. As Friederici comments (personal communication). "The 2002 paper model is based on the empirical data then available, and the fact that there are no arrows linking on-line processes to working memory represents the state of the art at that time. There were separate data on working memory activation and data on on-line processes, but not on their interplay". Given this, a future challenge is to understand how detailed modeling can offer hypotheses that build on more recent empirical data to achieve some measure of causal completeness at the neural or schema network level and then offer ideas for new experiments.

Turning to the cortical regions flagged in Fig. 2 (see Friederici, 2002, for the primary references), Friederici notes the classical view that Broca's area is the locus of syntax but argues that increased fMRI activation of BA 44 is triggered by syntactic memory but not by complexity, whereas local phrase-structure building seems to recruit the inferior tip of BA 44. Such conclusions, however, are based on the structure of the sentences to which subjects are exposed, not on an explicit computational model of parsing. Studies investigating semantic processes at the sentence level report a variety of activation loci, including the left inferior frontal gyrus (IFG, comprising BA 45/47), the right superior temporal gyrus (STG, which includes BA 22) and the left middle temporal gyrus (MTG, which includes 21 and 37) as well as the left posterior temporal region. However, activation of BA 45/47 appears to depend on the amount of strategic and/or memory processes required.

Friederici (2011) updates this analysis in light of recent data. She shows how the right hemisphere processes prosody as a complement to the syntactico-semantic processes of the left hemisphere, citing data showing that pitch discrimination in speech syllables correlates with increased activation in the *right* prefrontal cortex, violations of pitch for lexical elements in a tonal language modulate activity in the *left* frontal operculum adjacent to Broca's area, and processing of suprasegmental prosody involves the *right* superior temporal region and fronto-opercular cortex. Other data suggest that right hemisphere prosodic processes can influence left hemisphere syntactic processes. However, such extensions are outside the scope of this paper, and we will focus on the left hemisphere processes shown in Fig. 2. In what follows, the term "the 2002 model" will refer to the model shown on the right side of Fig. 2 in which the contributions of working memory are not made explicit, and the flow of information is purely feedforward (the downward arrows of Fig. 2).

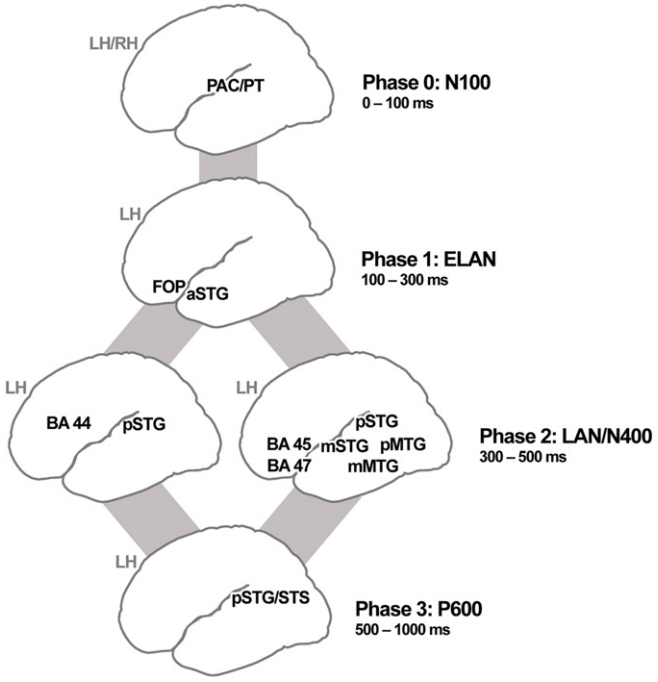

Fig. 3. Five modules and four processing phases extracted from the 2002 model and implemented within Synthetic ERP. The cortical regions depicted within each of the five modules are left lateralized, except for those generating the N100. Two language modules supporting linguistic processing and ERP generation are activated during Phase 2 (LAN shown at left; those for N400 shown at right). Abbreviations: LH, left hemisphere; RH, right hemisphere; BA, Brodmann's area; PAC, primary auditory cortex; PT, planum temporale; FOP, frontal operculum; aSTG, anterior portion of the superior temporal gyrus; pSTG/STS, posterior portion of the superior temporal gyrus and superior temporal sulcus; mSTG, middle portion of the superior temporal gyrus; pMTG, posterior portion of the middle temporal gyrus; mMTG, middle portion of the middle temporal gyrus.

2.2. Data on functional anatomy

In recent work, Friederici (2011, 2012) describe a predominantly left-lateralized temporo-frontal network of cortical regions that support various stages of syntactic phrase structuring and semantic integration. Regions are defined using a combination of PET, fMRI, inverse MEG source modeling, and lesion studies. In addition, functional parcellation schemes are devised for some of these regions based upon DTI tractography (Raettig, Kotz, Anwander, Friederici, & von Cramon, 2007) and Granger causality mapping of DTI and fMRI data (Upadhyay, Silver, Knaus, Lindgren, & Ducros, 2008).

In what follows, we use the term "module" for any group of brain regions or subregions postulated to work together in some subfunction of (language) processing. The model shown in Fig. 3 provides the neuroanatomical basis for the 2002 model by defining five functional language modules composed of cortical regions in the perisylvian language areas and connected via four major white matter fiber tracts (Friederici, 2009). We add a number of post-2002 references, and note that some of their data suggest modifications in the 2002 module but reiterate that such refinements are extraneous to our current goal, the grounding of the method of Synthetic ERP.

The first module (Phase 0, N100, around 100 ms) is subserved bilaterally by the primary auditory cortex (PAC) and the planum temporale (PT). These areas are thought to support the analysis of phonemes (Binder, Frost, Hammeke, Bellgowan, & Springer, 2000; Pantev et al., 1988). Bridging the Sylvian fissure, the next module (Phase 1, ELAN, peaking between 100–300 ms post stimulus onset) is considered responsible for phonemic concatenation (DeWitt & Rauschecker, 2012) and incorporates the anterior STG and the

frontal operculum connected by the ventral uncinate fasciculus. The posterior STG (pSTG) along with BA 44 comprise a module (Phase 2, LAN occurring in the 300–500 ms window) through connections mediated by the dorsal pathways through the arcuate fasciculus and the superior longitudinal fasciculus. This module is thought to be involved in syntactic processing (Kuperberg, McGuire, Bullmore, Brammer, & Rabe-Hesketh, 2000; Newman, Lee, & Ratliff, 2009). The most distributed module (Phase 2, N400, around 400 ms) is claimed to process semantic information and incorporates middle and posterior portions of the STG, middle and posterior portions of the MTG, BA 47, and BA 45 (Vigneau, Beaucousin, Hervé, Duffau, & Crivello, 2006) connected by the ventral extreme capsule fiber systems (Weiller, Bormann, Saur, Musso, & Rijntjes, 2011). Lastly (Phase 3, P600, around 600 ms post stimulus), the integration of syntactic and semantic information is carried out by a module including the pSTG and posterior superior temporal sulcus (pSTS), as well as the basal ganglia. Thalamic contributions to these stages of language comprehension have also been explored (David et al., 2011; Wahl, Marzinzik, Friederici, Hahne, & Kupsch, 2008), but are not considered in the current approach.

The 2002 model and its later iterations explore a larger body of cortical and subcortical language-related regions, but only those directly associated with the generation of linguistic ERP components were selected for Synthetic ERP implementation. However, future "doubly causal modeling" (i.e., using neural and schema networks to explain single cell data and behavior as well as to drive a forward model to generate ERPs) will have to take, e.g., thalamic and basal ganglia activity into account, as indeed we have done in our classic model of control of saccadic eye movements (Dominey & Arbib, 1992; Dominey, Arbib, & Joseph, 1995).

3. The two phases of Synthetic ERP: A preliminary computational framework

Synthetic ERP is a means to use computational models of neural or schema networks to predict the scalp potentials associated with ERPs. The method has two phases:

Phase 1: To generate amplitudes for dipole distributions from processing models for neurolinguistics based on neural networks or schema networks;

Phase 2: To apply forward modeling, based on a realistic anatomical model of the human brain and head, to compute Synthetic ERP activity which can be tested against available ERP data.

Later in the paper, we offer a preliminary perspective on Phase 1, but it is Phase 2 that receives detailed attention, and computer simulation, in the remainder of the paper. The present section offers a preliminary theoretical framework that makes explicit some key computational issues to be tackled in order to express ERP and localization data in a form which makes it a target suited for the Synthetic ERP methodology.

3.1. A preliminary framework

Let us use $[T_1(A), T_2(A)]$, etc., for the period during which region A is posited to make its contribution to the current epoch of processing. The nature of such contribution in the general information processing scheme depends on the hypotheses made by a given model. This is roughly the period during which the region's activity contributes to the ERP. In formalizing the data, we seek to assign a dipole amplitude time course to the region A for that interval,

$$d_A : [T_1(A), T_2(A)] \rightarrow d_A(t)$$

which assigns to each time t the amplitude $d_A(t)$ of the dipole oriented in the direction orthogonal to the cortical surface of A, and related to the synaptic activity of pyramidal cells. (More generally, we may need to use multiple dipoles, rather than one depending on the size of the region. More on this in later sections.) The forward model then computes the electric field as a function of time resulting from such current dipole activity. This method can be applied to all the relevant regions and the electric fields generated by their respective activities can be added to yield the complete ERP for that epoch (on this additive nature of the field, see Section 4.3).

The precise definition of the function d_A will be the focus of Phase 1. However, the current general specifications of d_A already imply that neural network (and schema network) models must incorporate the following constraints: (1) They must be tied to the 3-dimensional geometry of the cortex in order to derive the location and orientation of the dipole, (2) They should subdivide their neuron models into different cell-types that allow the read out of synaptic activity from pyramidal cells only.

In many ERP studies of language processing, the epoch starts with the onset of presentation of a word. In a *feedforward* model such as the 2002 model, it is assumed that the state of the brain at the start of the epoch may be ignored with one exception — that knowing whether the word is semantically or syntactically anomalous yields different values for d_A in some brain regions.

(a) In cases of divergent feedforward processing (i.e., a region receives input from at most one other region, and there are no loops), the timing in a chain $A \rightarrow B \rightarrow C$ goes something like this:

$t(A)$: time required after receiving coherent input for A to reach a degree of confidence for its processing of the current data.

$t(A \rightarrow B)$: time required for a coherent output from A to affect activity in B.

$t(B)$: time required after receiving coherent input for B to reach a degree of confidence for its current processing.

$t(B \rightarrow C)$: time required for a coherent output from B to affect activity in C.

Here $T_1(A) = 0, T_2(A) = t(A); T_1(B) = T_2(A) + t(A \rightarrow B); T_2(B) = T_1(B) + t(B)$, etc.

(b) In general, feedforward processing might involve confluent inputs, so that C receives input from A and B. In this case, a descriptive model might allow one to conclude that C can carry out its computation with the input from either A or B alone, or C might require both inputs. In the first case

$$T_1(C) = \min[T_2(A) + t(A \rightarrow C), T_2(B) + t(B \rightarrow C)]$$

and in the second case

$$T_1(C) = \max[T_2(A) + t(A \rightarrow C), T_2(B) + t(B \rightarrow C)]$$

but many other cases could be considered.

(c) However, even more generally there will be loops in the computation and it may well be that in simple cases a region C can complete its computation in feedforward mode, whereas in other cases it may need to get further input both bottom up (this is like a switch from the first case to the second in (b)) and top down — and this may involve input from regions encoding states achieved in processing earlier words of the input, and interaction between states "at multiple levels" initiated by receipt of the current word.

The 2002 model is a case of divergent feedforward processing. Later models by Friederici et al. have slightly relaxed this serial requirement, adopting a cascade type model which allows for some parallel activity and temporal overlap[1] (Friederici, 2012;

[1] Such overlap can be found in the processing of semantic and verb-argument information (N400) and morphosyntactic information and thematic role assignment (LAN) which is portrayed as occurring partly in parallel during Phase 2 of the 2002 model (see Phase 2 of Fig. 3).

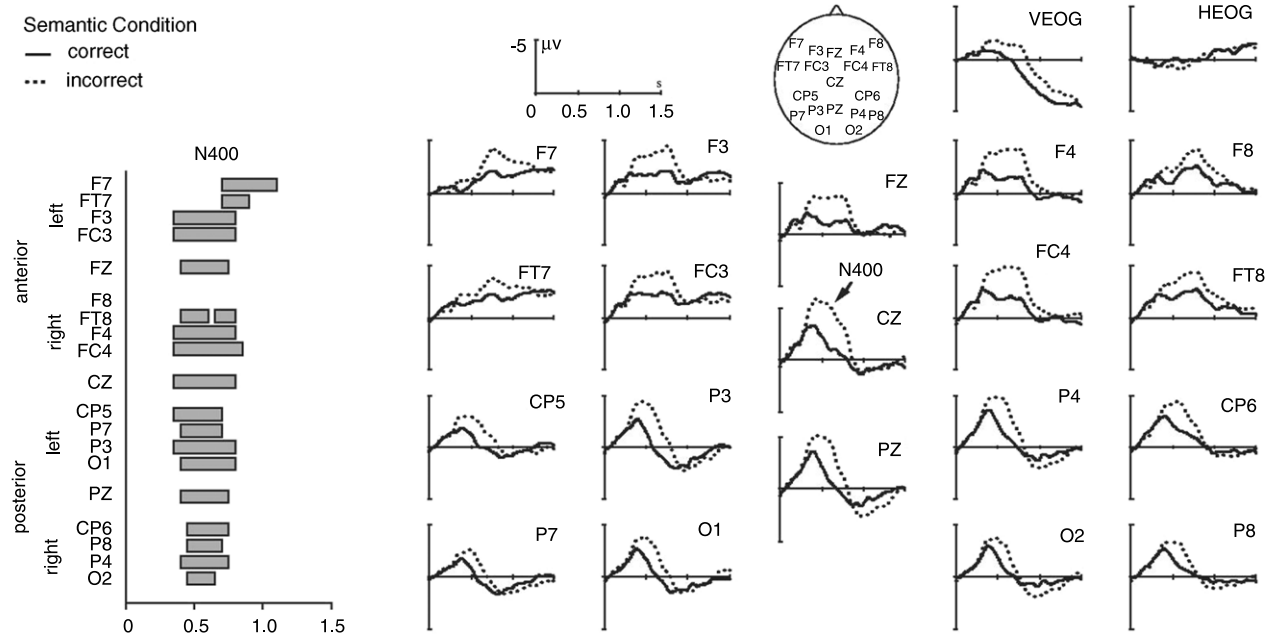

Fig. 4. Grand average ERPs when participants judged sentences for overall correctness, with averages calculated relative to a 100 ms post-stimulus onset baseline. The display shows ERPs for the semantic violation condition (e.g. 'Der Vulkan wurde gegessen' — 'The volcano was eaten') as compared to the correct condition (e.g. 'Das Brot wurde gegessen' — 'The bread was eaten'), where in the examples the origin of the *x*-axis corresponds to the onset of gegessen and negative voltage is plotted upwards. The rectangles at left display the results of MANOVAs comparing the incorrect condition to the correct condition for each electrode, starting at the onset of the participle. Shaded bars indicate significant effects ($p < 0.05$) whenever two or more successive 50 ms windows revealed a reliable effect.
Source: Adapted from Hahne and Friederici (2002).

Friederici & Kotz, 2003). It is our conviction — going back to the "neuralization" (Arbib & Caplan, 1979) of the classic HEARSAY model of speech understanding (Erman, Hayes-Roth, Lesser, & Reddy, 1980; Lesser, Fennel, Erman, & Reddy, 1975), and reinforced by current computational modeling — that the general models of case (c) are the rule rather than the exception, and it is this which motivates the need for Phase 1 of Synthetic ERP — using detailed processing models to infer dipole activity $d_A(t)$ for diverse cortical areas A in cases where complex interactions underlie the response to different task conditions. Such a model would yield individual trial-by-trial ERP values, but would then be averaged appropriately across an ensemble to yield predictions to be tested against the empirical data.

3.2. The challenge of timing data for the 2002 model

To illustrate the distinction between the *descriptive time course* of the 2002 model and the *generative time course* needed to implement a computational framework for Synthetic ERP, consider the N100 component which signals the acoustic processing of Phase 0. At the conceptual level it is enough to point out that the waveform peaks around 100 ms and thereby establishes the time window for phonemic processing ascribed to the bilateral primary auditory cortices by MEG (Pantev et al., 1988) and fMRI (Binder et al., 2000). However, the N100 component is not monolithic, so that the early phonemic processing stage could be better characterized by a combination of temporally and functionally distinct subcomponents with putative sources in *and around* primary auditory cortex (Naatanen & Picton, 1987; Scherg, Vajsar, & Picton, 1989). McCallum and Curry (1980) described three such subcomponents; N1a generated bilaterally in the auditory cortex on the dorsal surface of the temporal lobes with a fronto-central peak at around 75 ms, N1b a component of indeterminate neural origin peaking at the vertex electrodes around 100 ms, and N1c generated in the STG with a laterally distributed peak around 150 ms. A similarly complex cascade of cortical activation is implicit in other components such as the N400 (Kutas & Federmeier, 2011). While in this cautionary mode, consider the N400 of Fig. 1(a). It has been described as a small negativity around 400 ms that relates to a semantic anomaly. (There are other linguistic correlates as well, but they need not detain us here.) However, what we really see is a small N400 when there is no anomaly, and an N400 which lasts longer and rises higher when there is a semantic anomaly. Thus a computational model adequate for Phase 1 would not simply turn a dipole on if there is a semantic anomaly, but would rather show in some detail how semantic processes which are employed normally will be placed under stress when a semantic anomaly occurs, and then show how that translates into a time course for dipoles that forward modeling (Phase 2) can then use to explain the variation in N400 timing and magnitude seen in Fig. 1(a).

To further highlight the challenges of Synthetic ERP simulation, consider Fig. 4 which shows one portion of the ERP results from a study (Hahne & Friederici, 2002) which provides an experimental basis for Friederici's syntax-first serial approach to neurolinguistics and the resulting time course of the 2002 model. The challenge for Synthetic ERP is not simply to produce a single waveform as shown in Fig. 1 (the N400 arrow in Fig. 4) but also to obtain, to some acceptable degree of approximation, the distribution of activity seen across the various scalp electrodes. Note particularly the shaded rectangles at left of Fig. 4 which show for each electrode the time interval during which there is a significant difference between the incorrect and the correct condition. Our point is that, interesting though such an analysis of significance may be, our concern is to relate ERPs to a model of the underlying processing, and for this it is the actual waveforms in the two conditions that must be predicted (to some level of fidelity), not just the time course in which the stated difference is significant.

Timescales of activation must be much more clearly delineated than was required in synthetic PET and fMRI. Whereas the low temporal resolution of fMRI tends to superimpose all stages of activation and communication within an active module of cortical

regions, the instantaneous temporal resolution of ERP signals necessitates that signal resolution and propagation effects be taken into account. Signal propagation effects can be attributed to white fiber conductivity delays which can range from 10–50 ms (Aboitiz, Scheibel, Fisher, & Zaidel, 1992; Matsumoto, Nair, LaPresto, Najm, & Bingaman, 2004). We are confronted with a situation where signals are clearly propagating through the different elements of the 2002 model's temporo-frontal language network well before those regions contribute the ERPs with which their functions are associated. In this case, the conduction delays of feedforward signal propagation are inadequate to explain what is going on. For this reason we earlier introduced equations like $T_1(B) = T_2(A) + t(A \rightarrow B)$ to emphasize that propagation delays sum with processing time in a region before it achieves a coherent output that affects other regions. Such processing time should incorporate constraints on the temporal characteristics of post-synaptic potentials buildup and their impact on the activity profile of a brain region. Matsumoto et al. (2004) measured conduction delays between Wernicke's and Broca's areas of 22–36 ms, but conjectured that the early end of that response window, mediated by the thickest fibers, may have been lost due to an artifact in the recording data, thereby bringing the average latency closer to the 20 ms window previously mentioned. This ∼20 ms conduction delay is also in accordance with evaluations of white matter fiber conductivity (Waxman & Swadlow, 1977) and anatomical properties (Bishop & Smith, 1964). Thus the present implementation of Synthetic ERP will assume a 20 ms propagation delay prior to the onset of each processing phase. Later iterations will explore a more nuanced conduction delay scheme.

4. Phase 2 in detail: From areas of cortical activity to ERPs

We now turn to a detailed presentation of Phase 2 of the Synthetic ERP model, showing what is required to specify the cortical regions involved in a task with sufficient accuracy to allow first the computation of dipole sources, and from there of observed ERPs. We will use the 2002 model to make these challenges explicit when detailed computation of the forward model is invoked.

4.1. Forward modeling in the Synthetic ERP framework

Precise forward modeling requires both a head model and a processing model. The head model requires head meshes to define the various compartments of the head and a realistic brain mesh associated with a brain atlas to anatomically localize the brain regions. The head model also provides the conductivities of the various head volumes through which the electric field propagates. The realistic brain mesh enables one to anatomically constrain the direction and orientation of the dipoles associated with each cortical region or patch while the head meshes allow one to specify the various conduction volumes as well as the locations of the sensors on the scalp that simulate the EEG electrodes.

In what follows, we use dipole source waveform activations partially derived from the ERP empirical results, leaving open the future use of detailed neural or schema network models (as specified in Phase 1 of the full Synthetic ERP approach).

4.2. Head model

4.2.1. Conduction volumes

The implementation of Phase 2 of Synthetic ERP reported here uses a 4-compartment head model based on the MNI Colin27 MRI scans (Evans et al., 1993; Mazziotta, Toga, Evans, Fox, & Lancaster, 1995) which provides meshes representing the surfaces defined by the gray matter, the inner skull, the outer skull, and the outer surface of the scalp respectively. The reader unfamiliar with such models can refer to Appendix C which offers additional details. In addition, Appendix A provides the general physical formulation of the forward problem. We want to note that we use a realistic head model representing the anatomy of a specific individual. The impact of the model's specificity on conduction volumes is often neglected (many forward solutions go as far as simplifying the conduction volumes by concentric spheres). However, this specificity becomes an issue when considering individual-specific variations in cortical geometry (Mangin, Jouvent, & Cachia, 2010) as well as contrasts between, geometrically, functionally, or cytoarchitectonically informed approaches to defining brain regions (Fischl, Rajendran, Busa, Augustinack, & Hinds, 2008). Idiosyncratic anatomical variations of language-related brain regions should be considered as well (Amunts & Zilles, 2012; Keller, Crow, Foundas, Amunts, & Roberts, 2009; Keller et al., 2007). Such issues have long been recognized as important to neurolinguistics in general (Whitaker & Selnes, 1976), and take a central position here as the accuracy of ERP simulation critically depends on accurate representations of cortical folds. For this reason, in adjunction to the head model, we next discuss cortical parcellation ontologies and atlases. We want to insist on the need to quantitatively link EEG sources to standard brain nomenclatures in order to bring issues related to cortical geometry into computational modeling.

4.2.2. Brain areas

A brain area is a patch of cortex defined as a set of faces taken from the realistic brain mesh. Such an area can be defined as anything from a single mesh face to a whole brain region. Currently, Synthetic ERP lets one define brain areas by selecting an individual face or a set of contiguous faces using the Destrieux (Destrieux, Fischl, Dale, & Halgren, 2010; Fischl, Van Der Kouwe, Destrieux, Halgren, & Ségonne, 2004) anatomical atlases based on its Brainstorm versions. Although other atlases exist (we also implemented the Desikan–Killiany atlas (Desikan, Ségonne, Fischl, Quinn, & Dickerson, 2006), we mainly use the Destrieux nomenclature which defines regions based on gyral and sulcal borders (while the Desikan–Killiany cortical atlas defines regions based on gyri alone), giving us more flexibility. Selecting a region triggers the selection of all the vertices and faces of the realistic brain mesh that belong to this region (see Fig. 5). We incorporated the possibility of selecting only the anterior, middle, or posterior portions of an atlas based brain region. These informal subdivisions heavily used in conceptual models are defined as covering a third of the length of the area along its main axis as defined by PCA.

We apply our cortical brain atlas on the brain model of a specific individual. This approach reflects the limitation that most ERP data reported in the literature omit related data concerning the cortical anatomy of those individuals participating in the study. In addition most ERP components reported are averaged over a given population, begging the question of what is a good definition of the cortex's "average" geometry. In this paper we make explicit our choice of using a standard individual brain in order to insist that any discussion on ERP forward modeling must address issues related to cortical surface templates, variation in cortical geometry, surface averaging, and parcellation ontologies. For a review of the state of the art and challenges related to these questions, we refer the reader to Evans, Janke, Collins, and Baillet (2012).

4.2.3. Dipoles

Current equivalent dipoles are used to model the electromagnetic field sources associated with a given brain area. In the simulations reported below we consider mainly excitatory synaptic inputs (positive amplitudes for dipoles oriented inward).

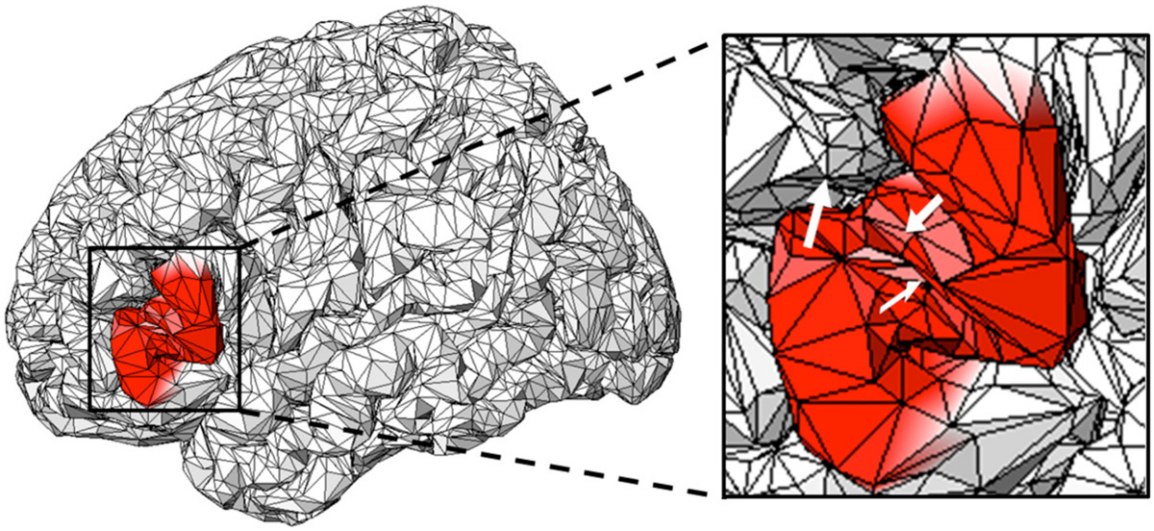

Fig. 5. (Left) Left pars triangularis (Desikan–Killiany atlas) brain area defined on the realistic brain mesh. Brain areas can be defined as individual faces or as brain regions. The Destrieux or Desikan–Killiany anatomical atlases can be used to select a collection of faces associated with a brain region or other cortical area. The current model uses the Brainstorm default version of these atlases. Each brain region is directly defined as a list of associated vertices on the MNI Colin27 brain mesh. (Right) Close up view of the brain area. The orientation of source dipoles is defined by the unit vector normal to the face and pointing inward. Here we show the normals to three arbitrary faces of the left pars triangularis (though for ease of representation, the normals are here oriented outward). The orientation of a source dipole within a given brain is highly dependent on its position.

Appendix B offers more details concerning the modeling of neural activity using current equivalent dipoles.

A key assumption of Synthetic ERP is that dipoles are constrained *both in position and in orientation* by the cortical geometry of the active source, thereby ensuring that all dipoles have a physical meaning (see Table 1). Appendix B details some of the hypotheses intrinsic to the dipole model regarding the curvature and size of the patch of cortex modeled. Synthetic ERP offers the option of summarizing a brain area by either a single dipole or as a distribution of dipoles associated with the faces of the mesh linked to the brain area. When a single dipole is used, its orientation is defined as the mean of the normal vectors associated with each of the faces contained in the brain area. The magnitude of the dipole at time t is given both by the surface S_A of the associated brain area and its time course function $d_A(t)$. S_A simply plays a role of multiplicative factor on $d_A(t)$ to ensure that the magnitude of a dipole is proportional to surface of brain tissue it represents. It is given by the sum of magnitudes of the normal to the faces contained in the brain area. The function $d_A(t)$ for a given dipole will link, in future work, to the activity levels in computational modules associated with the brain area this dipole covers (Synthetic ERP phase 1). In the present work, a more limited processing model is used to generate the time course activation function for each dipole.

4.3. Forward model and lead field computation

Synthetic ERP uses a standard method to compute the forward model using the FieldTrip (Oostenveld, Fries, Maris, & Schoffelen, 2011) MatLab implementation of OpenMEEG (Gramfort, Papadopoulo, Olivi, & Clerc, 2011). We refer the reader to Appendix E in which we offer an overview of the Boundary Element Method (BEM), the numerical method used here to solve the equations defining the electric field (detailed in Appendix A). Our key interest is to compute the lead field — the field observed at each sensor position. A computationally important characteristic of this field is that it can be expressed as the product of a gain matrix that only depends on the dipoles' positions and orientations with the vector representing the dipoles' amplitude (see Appendix D for an overview of this algebraic formulation). This implies that for a given set of anatomically constrained dipoles, expansive computation of the gain matrix needs only to be performed once. The EEG signal generated by a given time course of brain activity, modeled as variations in dipole amplitudes, can be then simply computed through one matrix multiplication.

4.4. Processing model

4.4.1. Defining dipole amplitude from a conceptual model

We now turn to the processing model whose role is to associate to each dipole a source waveform based on a conceptual model. As noted earlier the long term aim of Synthetic ERP Phase 1 is to infer these waveforms from an underlying neural or schema network model, but here we focus on an alternative problem: Given a conceptual model, formalize a set of quantitative hypotheses on the patterns of temporal activation within the brain and ultimately on the patterns of temporal activation of a set of dipoles. This then provides the input to forward modeling whose results may clarify places where the conceptual model is underspecified and thus specify more precise targets for Phase 1 building of computational network models.

We now focus on the five modules and four processing phases extracted from the 2002 model and shown in Fig. 3. It may be best to think of the graph of Fig. 3 as anatomical — showing pathways feeding information from one module to another — but in the case of a feedforward model like the 2002 model one could also interpret this as a graph of temporal precedence. However, this latter interpretation would not be applicable in models that include loops and top–down processing. The crucial point is to break down each module into brain areas or even finer subdivisions of cortex and to specify the time course d_A of dipole activity for each area so defined. At this level, it becomes irrelevant whether an area A so specified occurs in one module or many, and whether it is active once or many times during the overall task.

4.4.2. Activity modeling

Most conceptual models based on ERP results directly associate the activation time of a brain module by appealing (perhaps implicitly) to the boxcar representation critiqued in our discussion

of Fig. 4. In order to show the strengths and limitations of such an assumption, we choose in the present model to directly link the d_A functions (dipole amplitude waveforms), for the brain area A associated with a given brain module, to the shape of its component within the associated ERP. However, the shape of an ERP component is not always readily accessible from the EEG literature which tends to emphasize the time of occurrence, duration, and size of the component — and these values can be reported in a variety of ways, but there is no consensus (Luck, 2005). Moreover, our concern here is to lay the foundations for linking ERP data to detailed models of underlying processing. As we have stressed elsewhere (Arbib et al., 2000), the fact that area A is "significantly more active" in task X than area B does not mean that there is no activity in area B during task X. A processing model will provide an account of the time course of detailed neural or schema activity in both areas A and B during the task, however ERP results are usually presented without assessing the presence of possible overlaps between components. This makes the quantitative extraction of the shape of a component difficult.

To clarify the issues here, we suggest a means to extract the N100 component generated during an auditory oddball detection task from the empirical measurement reported by Scherg et al. (1989) from an overall ERP waveform. The challenge is to hypothesize what part of the empirical data given by the solid curve in Fig. 6 is actually the N100 component, and what parts of the waveform are extraneous to this module. We took the original waveform and defined the duration time D of the N100 component as the full width at half the extremum of the peak at 100 ms, spanning the interval $[T1, T1 + D]$. We then modeled the shape of the peak by finding the gamma function γ defined on [0, 1] and normalized in amplitude such that $\gamma((t-T1)/D)$ results in the best fit for that duration (parameters for γ are $k = 4$ and theta $= 0.1$). From there, d_A associated with the N100 brain module is defined as $\gamma((t-T1)/D)$ for t in $[T1, T1+D]$. Once we have defined the N100 component in this way, the difference between the posited N100 and the actual ERP activity in Fig. 8 is then hypothesized to correspond to neural activity in other brain regions. We do not claim that a gamma function is the only option for the fitting of an ERP. It has the property of being defined on the positive real line with $\gamma(0) = 0$ for a certain range of parameters. This fits with the assumption that the activity of a brain area has an onset time before which its activity is null. However a polynomial fit would of course also be possible but would leave the number of parameters unconstrained.

To generalize this example, recall that a brain module M is based on the hypothesis that certain brain areas are implicated in a specific function F. In a feedforward model, we may assume that a given area A is active only once and only in one module. In general, though, an area A may be involved in multiple modules. However, we here consider how to extract an estimate for $d_A(t)$ for the time period associated with the peak (P or N) of a strong deviation in the ERP associated with an anomaly in the execution of function F. Noting that most modules in Fig. 3 are each associated with several brain areas, we make (for now) the simplifying assumption that the same amplitude waveform is associated with each area linked to the given module. Given this, we start with an ERP waveform that has a significant peak posited to correspond to a particular ERP component. Then, just as before, we extract a duration from the peak, and then find the gamma function that best fits the peak during that duration. The resultant curve is our formally defined $d_A(t)$ for that interval for all areas A associated with the module for that component. Unfortunately, such curve fitting is inapplicable when the necessary details of the ERP waveform are not reported in the experimental literature.

Given our discussion of the N400 in Fig. 1, note that we are looking (at least) for the $d_A(t)$ for a given area of a given module in two different conditions, with and without the anomaly.

As noted at the beginning of this section, we do not claim that the modeling choices we made in order to extract d_A were the only ones possible. Our goal was to give a quantitative form to the assumptions underlying the interpretation of ERP components, often implicit in the neurolinguistic literature. The two main assumptions can be summarized in the following statements:

(1) An ERP component has a given qualitative shape. This shape is roughly the same for classes of components such as N100, N400, and P600.
(2) The shape of the ERP component is isomorphic to the activity of its underlying brain regions.

We formalize (1) quantitatively by choosing to model each ERP components with a gamma function (best fitted to each component). The direct association between such gamma functions and d_A formalizes (2).

We insist on the fact that such a phenomenological fit of the ERP data is *not* an intrinsic feature of Synthetic ERP but stems from a desire to formalize what we consider to be the way most neurolinguistic models interpret such empirical results. In doing so we seek a better understanding of how to link computational models to conceptual ones as well as identify the stumbling blocks that qualitative data formats might create for modelers (for a more general discussion of these issues and of the challenges posed to neuroinformatics by neurolinguistics see Arbib, Fagg, and Grafton (2003); Lee and Barrès (in press)). The goal of future work on Synthetic ERP Phase 1 is to simulated ERPs by applying the forward model to a realistic processing model of the interactions between neural components adequate to produce the observed language behavior.

5. Simulation results

We now present simulation results for a forward model computation of ERPs based on the 2002 model of language comprehension. We first detail the information extracted from the 2002 model (using the methods of the previous section) that served as the basis for the forward model. We then qualitatively compare the simulated scalp potential topographies generated by the forward model against empirical data (Simulation results 1: Scalp potential topographic maps). This enables us to highlight some initial issues related to source dipole localization. We finally move on to simulating ERPs based on the 2002 model (Simulation results 2: Synthetic ERPs) and compare our results with the ERP experimental data reported by Hahne and Friederici (2002) in Fig. 4.

5.1. Mapping the 2002 model onto cortical geometry

As in Fig. 3, the 2002 model defines five brain modules associated with the different phases of sentence comprehension each considered to be the source of a specific ERP component. The brain regions associated with these brain modules are referred to using a mixed ontology of gyrus/sulcus neuroanatomical landmarks along with cytoarchitectonically defined Brodmann areas and functionally defined sensory areas. We mapped these regions onto the Destrieux atlas that offers a cortical surface parcellation based on cortical geometry. We based the conversion on the description of the Destrieux atlas given by Fischl et al. (2004). The result of this conversion is presented in Table 2. Brodmann ontology is frequently used in neurolinguistics. However, given the sensitivity of the EEG sources to the gray matter gyral geometry, idiosynchratic variations in the gyral localization of Brodmann areas are a limitation to their usefulness in Synthetic ERP (see Amunts, Lenzen, Friederici, Schleicher, and Morosan (2010) for a discussion of these issues, focusing on Broca's area).

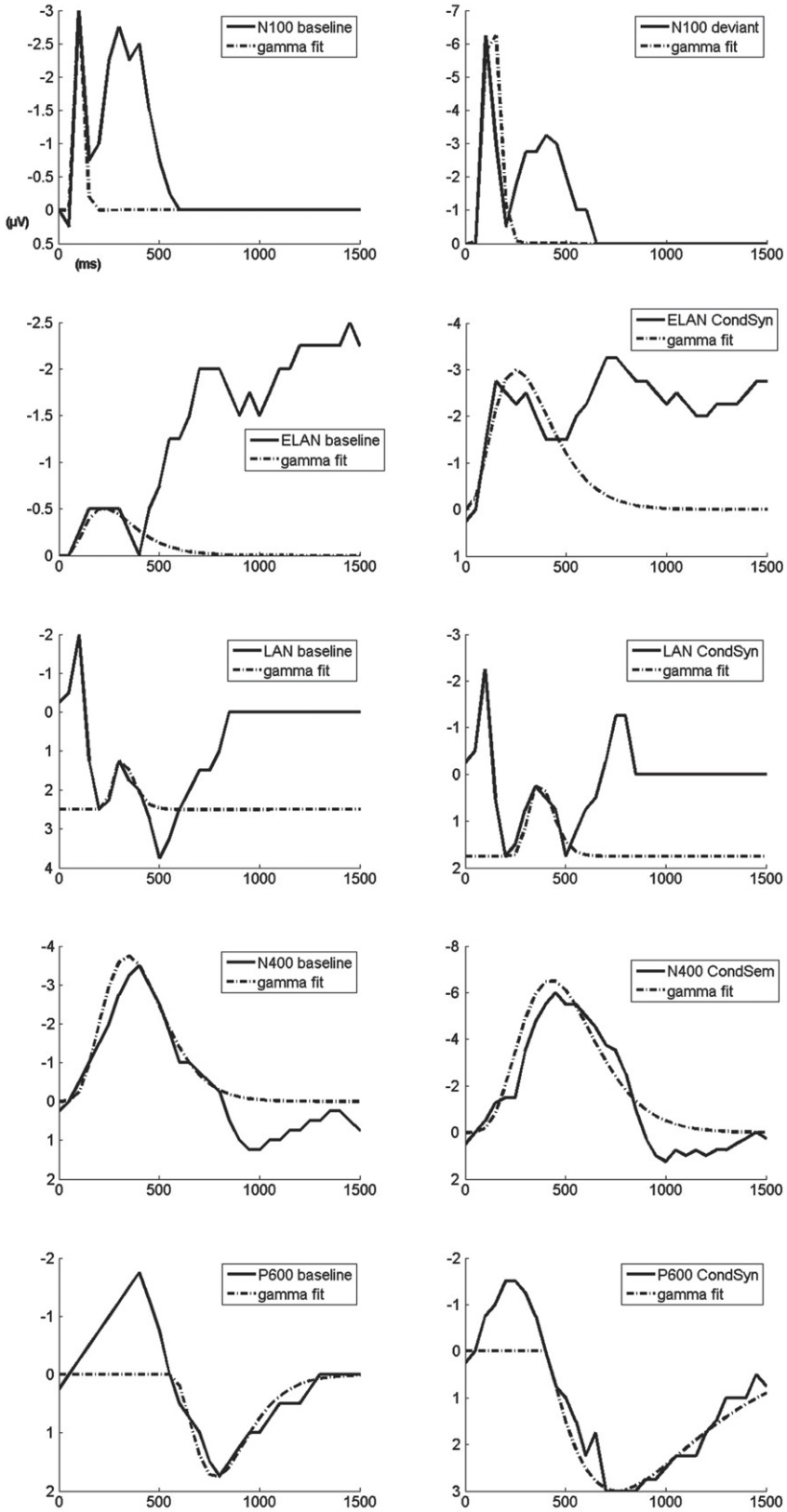

Fig. 6. d_A shape definition from the different ERPs. In each case, the solid black line represents the experimental ERP waveform while the semi-dotted line represents the best-fit result to the stated ERP component. Since N100 and LAN are not analyzed in their study, N100 is defined based on Scherg et al. (1989) and LAN based on Penke et al. (1997). Note that LAN presents a specific case where the component is a negative going deflection on a positive baseline value. CondSem refers to the semantic violation condition while CondSyn refers to the syntactic violation conditions. For the brain module source of any given ERP, the shape of d_A is defined as the best fitting gamma function associated with the peak for the stated component. For the actual d_A see Fig. 9.
Source: Data for ELAN, N400, and P600 are taken from Hahne and Friederici (2002).

Table 2
Conversion of the mixed brain ontology of the 2002 model into a single anatomical atlas, the Destrieux brain surface atlas.

Destrieux atlas		Friederici's model	
Hemisphere	Name	Cortical regions	Modules
Left & right	Anterior transverse temporal gyrus (of Heschl)	Primary auditory cortex	N100
Left & right	Planum temporale or temporal plane of the superior temporal gyrus	Planum temporale	N100
Left	Lateral aspect of the superior temporal gyrus [Anterior segment]	Left anterior STG	ELAN
Left	Opercular part of the inferior frontal gyrus	Left frontal operculum	ELAN
Left	Triangular part of the inferior frontal gyrus	Left frontal operculum	ELAN
Left	Opercular part of the inferior frontal gyrus	BA 44	LAN
Left	Triangular part of the inferior frontal gyrus	BA 45	N400
Left	Orbital part of the inferior frontal gyrus	BA 47	N400
Left	Lateral aspect of the superior temporal gyrus [Middle segment]	Left middle STG	N400
Left	Lateral aspect of the superior temporal gyrus [Posterior segment]	Left posterior STG	N400, LAN, P600
Left	Middle temporal gyrus (T2) [Middle segment]	Left middle MTG	N400
Left	Middle temporal gyrus (T2) [Posterior segment]	Left posterior MTG	N400
Left	Superior temporal sulcus (parallel sulcus) [Posterior segment]	Left posterior STS	P600

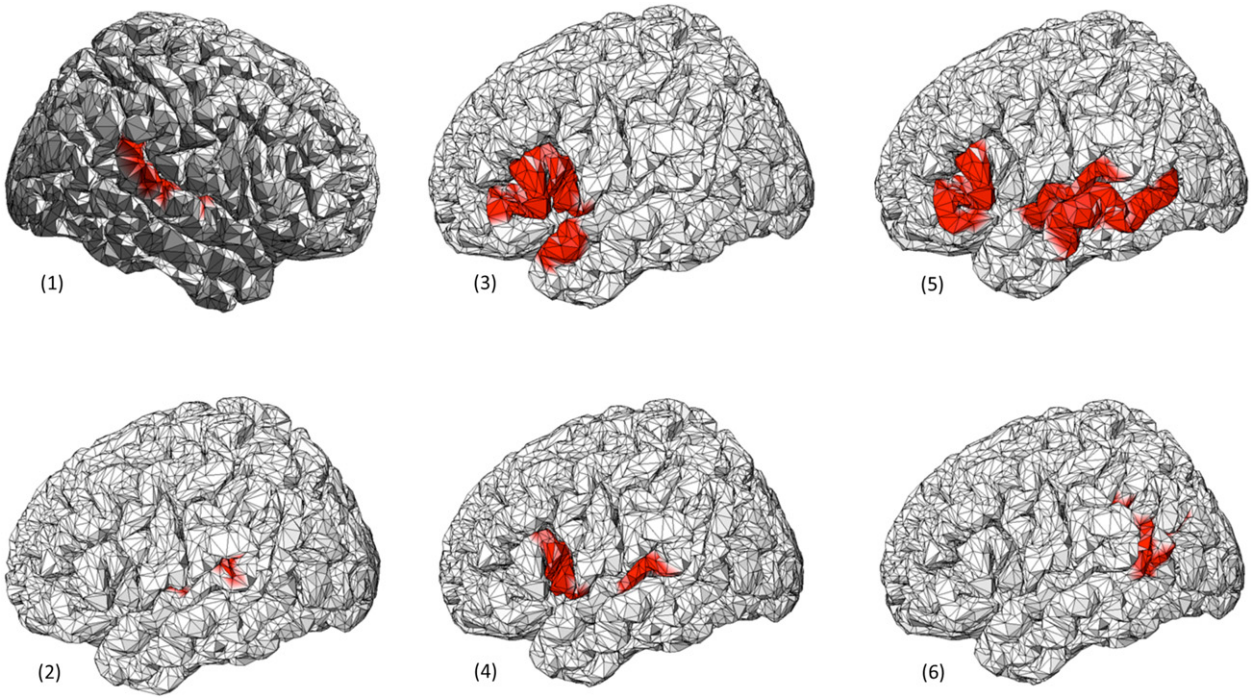

Fig. 7. Faces of the realistic brain mesh associated with the 2002 model in the head model for dipole localization. All the areas are defined using the Destrieux anatomical atlas. (1) & (2) N100 module. The bilateral Heschel's gyrus is not visible here. (3) ELAN module. (4) LAN module. (5) N400 module. (6) P600 module. (For the precise anatomical regions and their comparison with the 2002 model see Table 2).

Fig. 7 presents the faces of the realistic brain mesh associated with the different brain modules in the head model. Our definition of the LAN module is more extensive than in Fig. 3, because the 2002 model does not make precise what parts of the frontal operculum need to be included. We were able to include the anterior, middle, or posterior parts of the superior and middle temporal gyri as required by the 2002 model, but such regions do not have a standard definition and are therefore are not part of the Destrieux atlas. Finally, it is important to note that the 2002 model includes the basal ganglia in the P600 brain module but we do not include any subcortical structures in our current head model.

Single average dipoles were associated with each brain area which was part of at least one brain module. When simulating scalp potential topographies, the lead field was computed at every vertex of the top part of the outer scalp mesh. Otherwise, the Brainstorm 10/10 65 channels default electrode positions were used as computation points for the lead field. Conductivities were kept at the values defined by Oostendorp, Delbeke, and Stegeman (2000).

5.2. Processing model: Brain modules and activity timing

We use the connectivity defined in the graph of Fig. 3. Due to the *serial* nature of the 2002 model, *the connectivity is interpreted as a graph of temporal precedence*. For each brain module A, the activation times $T_1(A)$ ("on Time") and $T_2(A)$ ("off Time") are defined as follow. $T_2(A)$ is systematically defined as $T_1(A) + D(A)$ were $D(A)$ is the full width at half extremum of the ERP component associated with A. For the input module, N100 module representing the auditory sensory areas, the T_1 was set to 20 ms as the time required for the auditory input to activate these brain areas (Rupp, Uppenkamp, Gutschalk, Beucker, & Patterson, 2002). For the other modules, the T_1 was defined as the "off time" of the preceding module to which 20 ms were added to account for transfer delays. Other delays such as those inherent to the dynamics of neural computation (in particular post-synaptic potential buildup delays) are thought of as already lumped into the definition of d_A. Phase 1 will assess the requirements these impose on neural and schema networks. In the case of multiple inputs

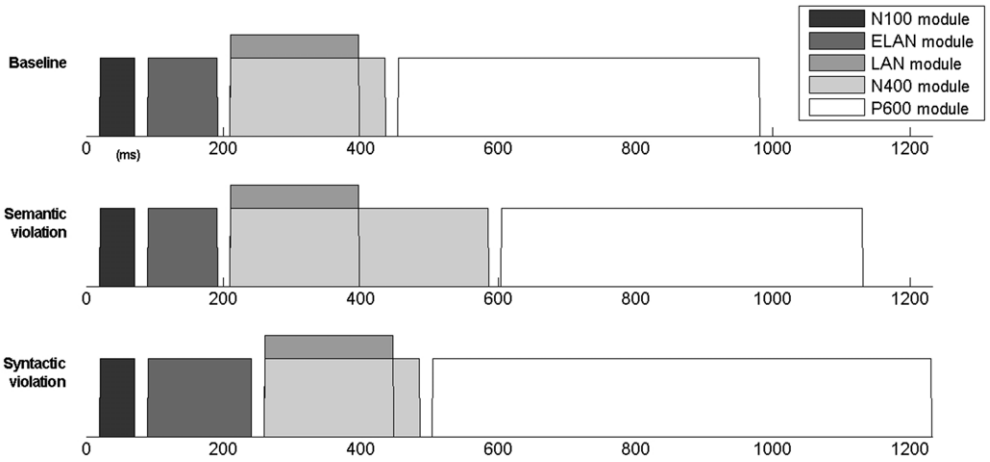

Fig. 8. Activation durations for each brain module for ERP component sources in the various experimental conditions. The durations of activity for each module were extracted from experimental data as the width of the respective component at half maximum. (LAN boxcar is shown higher so as not to be obscured by N400.)

(see P600 module), we made the assumption that both preceding processes needed to be done before the next process could start.

Activation times are given for each module and for each experimental condition in Fig. 8. In the semantic condition, only the activity of the N400 module changes duration from the normal condition following the reported effect of such violation on the N400 ERP. In the syntactic violation condition, both ELAN and P600 modules, activation times are affected since this violation triggers a change in the ELAN and P600 components (according to Hahne & Friederici, 2002). Fig. 9 presents the d_A associated with each brain module. They are given by the gamma functions extracted from the empirical ERP data as detailed in Section 4.4. However, to follow more closely the hypotheses made by the 2002 model, the onset of activity is now determined by the onset times we just discussed and not by the onset of the ERPs to reflect the serial computation hypothesis.

We do not claim to have the capacity to extract the exact timing of activations or activity level of brain modules from ERP but for now follow the general assumption that the ERP duration reflects the duration of the associated brain processes while the ERP amplitude reflects their activity levels. These claims are pervasive in neurolinguistics and the role of the present work is to show both their strength but also their limitations in the framework of Synthetic ERP. Once again, future work on Synthetic ERP Phase 1 will relax such assumptions since the timing of activations and activity levels of brain areas should then directly result from activity patterns of the neural or schema model.

5.3. Simulation results 1: Scalp potential topographic maps

For each ERP component, we now compare the scalp potential topography generated by simulation of the baseline level activation of its associated brain modules with an empirical measurement of the scalp potential topography. Each brain area composing a module is represented by a single dipole averaging its curvature and proportional in magnitude to the surface of the area. Appendix B makes explicit the fact that such an averaging would be an acceptable approximation of a brain region in a general case under the hypotheses that this region is small and that its curvature is negligible. The assumption we make here aims therefore at illustrating the problem often ignored by conceptual models that EEG sources need to be considered in their spatial extension – with the exception of very focal activities as in the case of an epileptic focus.[2] ERP components show variability in their associated scalp distributions just as they show variability in their shape, timing, and magnitude. However, this initial comparison enables us to get a first estimation of the validity of the simulations at the stage where the only assumption results from what could be extracted from the conceptual model concerning the neural substrates associated with each brain module.

As shown in Fig. 10, the simulated topographies did not qualitatively match the empirical ones for all the brain modules. In the case of the N100 module and the LAN module, the results are close to the empirical measurements with the following caveats. The N100 is more right lateralized. The maximum negativity is achieved for the electrode C6 as opposed to Cz for the empirical result. This asymmetry in our simulation could be due to the anatomical asymmetry of the bilateral brain areas defined as the sources of the N100 (see Fig. 7(1) and (2)). The topography for the simulated LAN is roughly correct with a negativity slightly posterior of the empirical one (minimum for electrode T7/T3 for the simulation compared with F7 for the empirical data). For ELAN, N400, and P600 the simulated topographies are blatantly incorrect. However, we could find for these a face in the anatomical region attributed to each brain module whose associated dipole yields a greatly improved potential topography. For ELAN the result is more left lateralized than in the empirical measurements. The same is true of the N400 simulated topography whose asymmetry differs from the overall symmetry of the empirical one. As for P600, once again the simulated distribution is shifted to the left side of the head compared to the empirical data. This general tendency to be left lateralized could reflect the absence of consideration of the role of the right hemisphere in language processing in the 2002 model. The N400 is the most obvious case and it has been reported that the right hemisphere plays an important role as a source of this component (Maess, Herrmann, Hahne, Nakamura, & Friederici, 2006).

This shows the importance of the careful consideration of the geometry of the cortical areas whose activity generates an ERP. A coarse anatomical definition of the brain areas associated with

[2] From a historical point of view, identifying an epileptic focus has been one of the driving forces behind the development of EEG source localization methods. This could partially explain why so much of the literature circles around modeling brain activity through the use of one or a few dipoles. This fits the hypothesis that only a few localized patches of cortex are generating the EEG signal during an epileptic seizure. However, it is clear that in the more general case — as in language processing — the number of cortical regions as well as their size would require to revise such view.

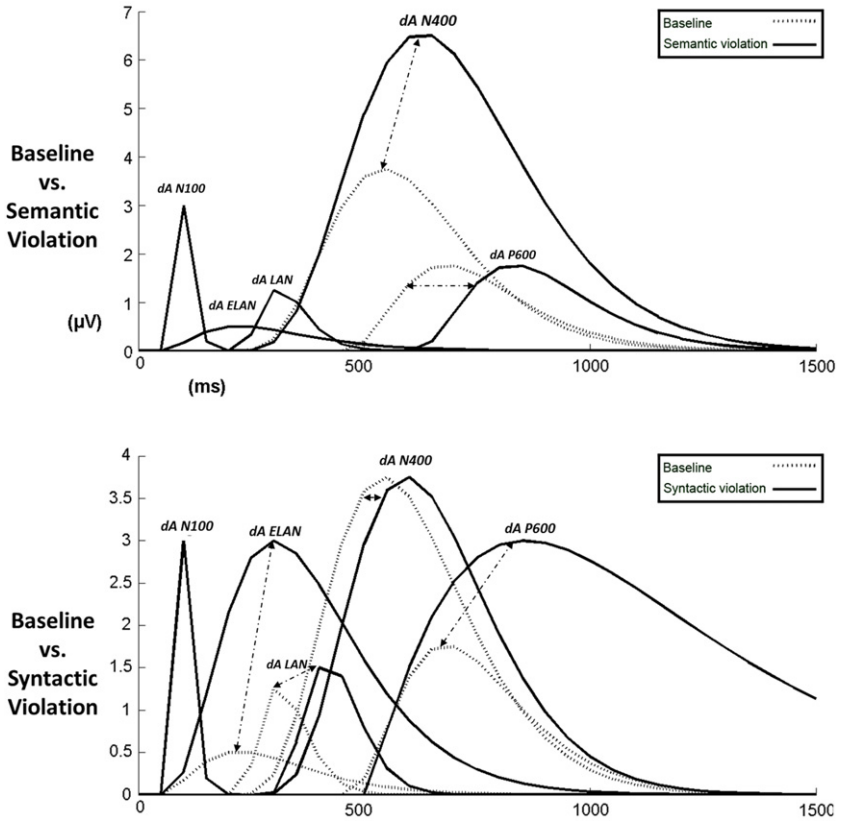

Fig. 9. d_A associated with each brain module for the three experimental conditions. In the semantic violation case, the d_A for the N400 module changes in duration and activation level. This triggers a change in onset time of the P600 due to the serial processing hypothesis. In the syntactic violation condition, the d_A for the ELAN changes in duration and activation level compared to control as well as P600. The change in ELAN duration impacts all the activations times downstream. (Note that the activation scale differs between the top and the bottom graph). Dotted arrows identify, when needed, d_A function associated with a same module.

a processing module in a conceptual model does not provide in most cases enough information to simulate an ERP-associated scalp potential topography. Although averaging the curvature of an area can give reasonable results, in most cases it is necessary to search for the correct cortical patch within an area whose curvature and position result in a field that fits the ERP empirical topography. It is important to note however that such a search differs from most of the inverse solution models that look for best fitting dipole localization and orientation without any anatomical constraints. Although insufficient, the brain modules defined in the 2002 model, once associated with a realistic mesh modeling the gray matters folds, considerably constrain the search space to a finite set of dipoles. A yet even more realistic approach would be to model brain regions by a distribution of dipoles over its surface rather than by a single dipole (in the spirit of Bojak et al. as described in 1.3). However, it will be the role of Phase 1 to analyze how to link a neural network representation of the distributed computation occurring in a brain region to a geometrically accurate model of cortical activity.

5.4. Simulation results 2: Synthetic ERPs

Given the preceding results, we modified the head model in the following way. For the N100 and LAN brain modules we kept their associated dipoles defined as average area dipoles. For the ELAN, N400, and P600 brain modules for which the average area dipoles gave incorrect scalp potential topographies, we kept the better fitting single dipoles described above. In order to keep the contribution of the areas comparable, the dipoles for all the areas (including the ones associated with the N100 and LAN brain modules) were given an equal magnitude. This is tantamount to saying that we remove the area surface factor and consider all the dipoles to summarize a patch of cortex of equal surface. In the case of the single average dipoles, that means that we kept the location and orientation but that the dipole is not thought to model the activity of the whole area but some distributed portion of this whole area.

We compare the empirical data extracted from Hahne and Friederici (2002) and our simulated ERP. For simplicity, we only consider here the empirical ERP time course as recorded at the most significant electrode (Cz for N400, F7 for ELAN, and Pz for P600). In the absence of noise in our system, we simply define our "most significant electrodes" as the ones where the maximum peak amplitudes for a given component are observed (TP7 for N400, F3 for ELAN, and PO3 for P600). Fig. 11 provides a visual representation of the differences of localization in the most significant electrodes between the empirical and simulated data. ELAN and P600 appears to be roughly maximal in the same scalp quadrant as for the empirical data (anterior left for ELAN, posterior left for P600). N400 maximum amplitude on the other hand is highly left lateralized in the simulated case when it is central in the empirical data. As mentioned in Simulation results 1, this could tie back to the assumption of purely left lateralized sources for N400. Future work should try and compare this result with those resulting from the inclusion of right lateralized brain areas as N400 sources as suggested by Maess et al. (2006).

From these comparisons, it seems that the level of precision one could expect from Synthetic ERP simulations should clearly be lower than the level of granularity of scalp regions provided by the 10/10 65 electrodes cap positions. In linking empirical reports of ERP to computational simulations, an average value over a few electrodes covering a standard brain region might be

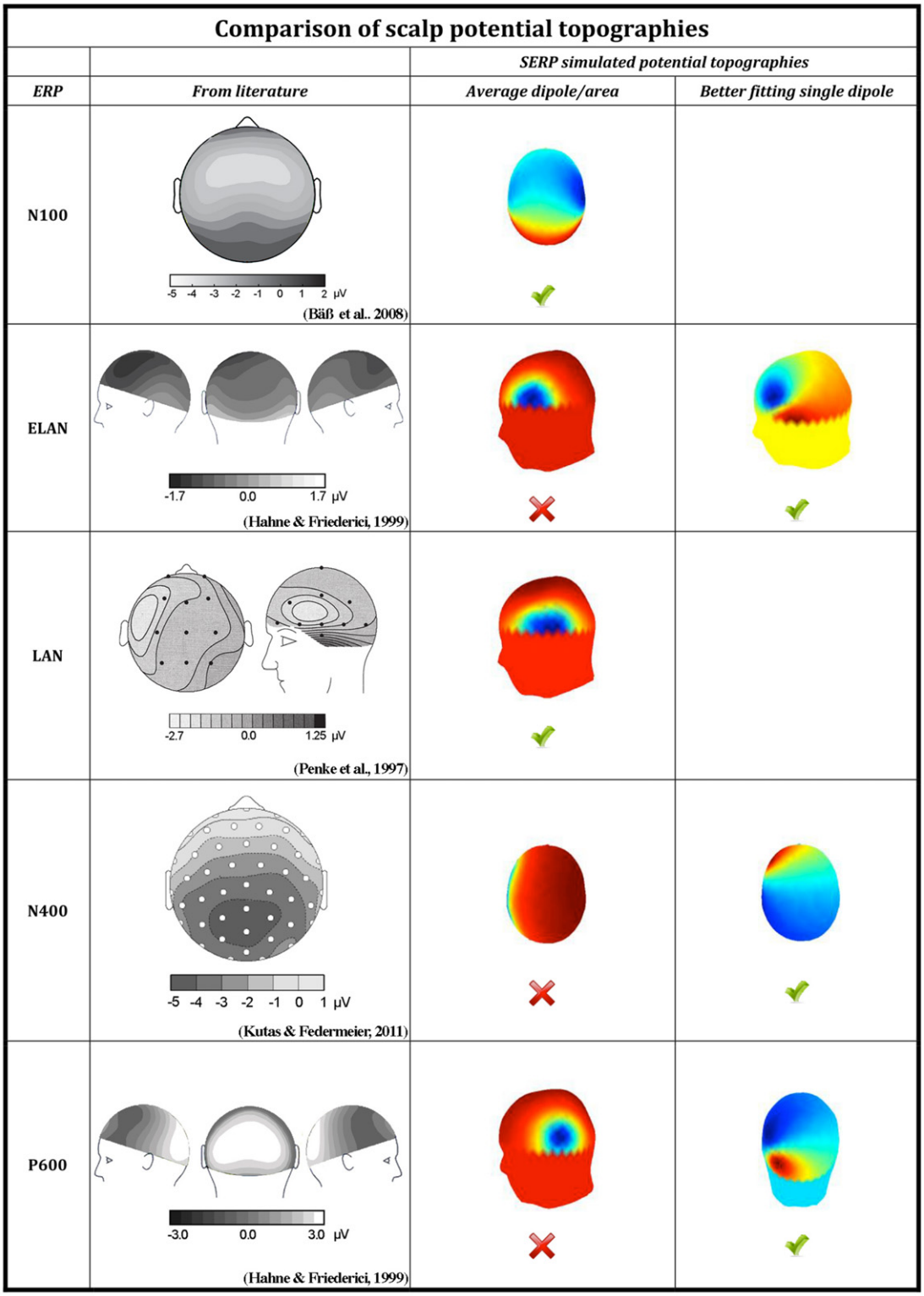

Fig. 10. Scalp potential topographies. Comparison of empirical data and simulated fields: Each row represents the data and simulation result for the ERP effect listed in the leftmost column. The second column from the left depicts the topographies of the potentials associated with the ERP as extracted from the literature (Bäß et al., 2008; Hahne & Friederici, 1999; Kutas & Federmeier, 2011; Penke et al., 1997). Rather than displaying waveforms as in Fig. 3, we display scalp potential topographies as smoothed "heat maps" for the moment at which a given potential reaches its peak. In the absence of a standard way to report these topographies, we did not try to find matching representations and the patterns should be taken as qualitative depictions. The two columns on the right present simulated scalp topographies based on the activation of the brain module associated with the ERP by the 2002 model (lower potential values in blue, higher in red). The "Average dipole/area" column present the simulated topographies based on single average dipole for each area. If the N100 and LAN components coarsely match the empirical data, ELAN, N400, and P600 topographies are incorrect. In the rightmost column, for these incorrect cases, we found a single dipole associated with a face belonging to a brain module whose resulting simulated topography fits qualitatively better with the empirical topography. (For interpretation of the references to color in this figure legend, the reader is referred to the web version of this article.)

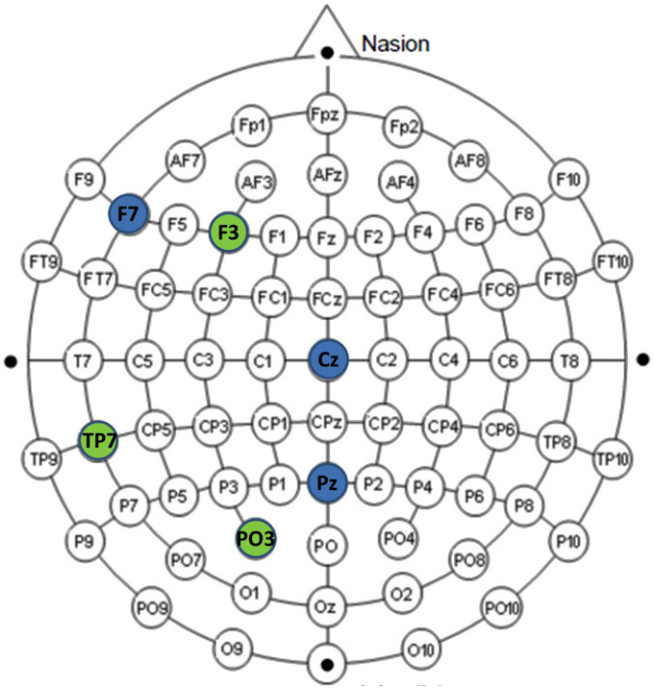

Fig. 11. Comparison of the empirically most significant electrode position for Hahne and Friederici (2002) (blue) and Synthetic ERP (green). For the empirical results, the most significant electrodes for the measurements of ERP are: F7 for ELAN, CZ for N400, and Pz for P600. In the case of Synthetic ERP they are F3 for ELAN, TP7 for N400, and PO3 for P600. If the simulated most significant electrodes for ELAN and P600 are roughly similar to their empirical counterparts, the case of N400 shows a clear left lateralization in the simulation absent from the empirical data (see discussion in Simulation results 1: Scalp potential topographic maps). (For interpretation of the references to color in this figure legend, the reader is referred to the web version of this article.)

more appropriate. This states the challenge both for Synthetic ERP phase 1 with a need to assess more precisely what the scalp localization precision could be. But it also should highlight the role computational Synthetic Brain Imaging endeavors could play in assessing what appropriate levels of representation of empirical results to provide suitable quantitative summaries for modelers.

Fig. 12 presents the comparison of the empirical ERP time course and the simulated ones based on our forward model. In both the empirical and Synthetic ERP case, the solid line represents the control time course while the dotted line represents the time course in the experimental condition mentioned on the right of the figure. Once again we did not aim at simulating the exact potential values but the relative variations between the baseline and the experimental conditions. These simulations raise the following issues.

Looking at the P600 simulation, the first clearly apparent result is that, if we replicate the late positivity, the temporal relation of the P600 component in the baseline and in the syntactic violation condition differs between the empirical and simulated results. Such a difference results from the fact that we did not directly choose the onset time of our brain module's activations based on the ERP but derived them from the serial processing hypothesis made by the 2002 model. As shown in Fig. 8, the onset time for the activation of the brain module hypothesized to generate the P600, given the hypothesis of serial processing, does not markedly differ between the baseline and the syntactic violation condition (interestingly such a difference in onset is clear however in the semantic violation condition). The only minor difference in activation times is due to the increase by 50 ms of the duration of the ELAN downstream which delays all the following processes.

Turning to the ELAN component, the simulation shows a large negative deflection peaking in a time window [100–300 ms] similar to the one presented in the empirical data. However, the general trend of negative going deflection displayed by the empirical time course in both baseline and syntactic violation conditions is not replicated. This points towards the limitations of our approach but also of the empirical reports of ERP results which tend to ignore some features of the measured signal that would however provide interesting benchmark cases for testing a modeling effort.

Finally, for the N400 the model does replicate the increase in duration and magnitude of the N400 component when contrasting the semantic violation condition to the baseline. If we abstract the large initial positive peak with results from the early activation of the N100 brain module, the shape of the empirical N400 is relatively well replicated, including the initial absence of noticeable difference between the anomalous and baseline conditions until 500 ms when a clear negative going deflection can be observed in the semantic violation condition.

6. From preliminary results to emerging challenges

By providing a first attempt to directly simulate ERP components by linking a neurolinguistic conceptual model to a forward model, we were able to make explicit some of the challenges raised by the attempt to link ERPs to the underlying dynamics of neural circuitry. These challenges are methodological, technical and computational, but they also reside in part in the way in which data are documented in the empirical literature. For example, in discussing Fig. 4, we emphasized the difference between, for example, assessing the timing of a dramatic increase in negativity in response to a semantic anomaly and seeking to understand the underlying processing of the meaning of a word which determines whether or not it is anomalous with respect to the fragment of a sentence that precedes it. Accordingly, Synthetic ERP should be understood as an essential tool for future efforts to link experimentally observed phenomena to detailed cognitive processing models, as well as an attempt to define what quantitative aspects of those phenomena will allow experimentalist and modelers to collaborate more effectively. The latter issue was highlighted by our distinction between the descriptive time course of activations provided by the 2002 model, and the generative time course we sought to articulate using the d_A functions. By simulating the dipolar contribution of different cortical regions on the basis of observed scalp topographies we were able to underscore the necessity for geometric definitions of cortical structures when seeking to link functional anatomy to neuroelectromagnetic phenomena.

As we discuss in more detail in Section 7, Phase 1 of Synthetic ERP will develop the necessary quantitative tools to extract d_A activation patterns from computer simulation of a neural or schema network model of the underlying language processing. Unfortunately, current network models of this kind are not structured with respect to hypotheses on the anatomical localization and orientation of different subnetworks in the three-dimensional head.

The present paper focused more on Phase 2 of Synthetic ERP, namely the development of a forward model capable of generating scalp-recorded EEG signals when provided with activities in defined regions of cortical anatomy. To initiate our analysis, we used a standard head model composed of four volume conductors. Field sources were modeled as source equivalent dipoles, sensor positions were given default values, and the forward computation of the field relied on existing boundary element method implementations. Rather than assess the effect of the various elements of the head model on the quality of the field's computation (Hallez, Vanrumste, Grech, Muscat, & Clercq, 2007; Wendel, Väisänen, Malmivuo, Gencer, & Vanrumste, 2009), we emphasized the impact of cortical geometry on source dipole modeling. Whereas inverse approaches to source localization from

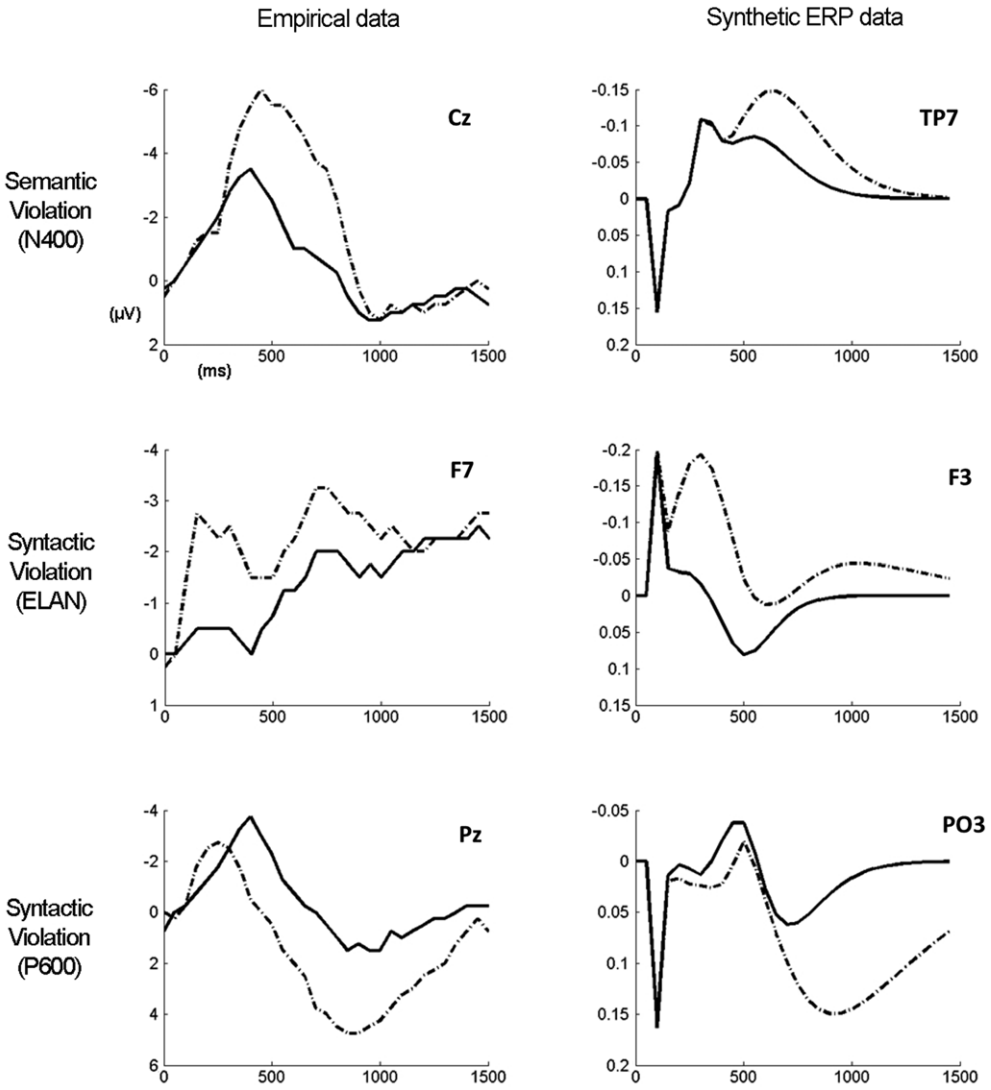

Fig. 12. Comparison of ERP time course as extracted from empirical data (Hahne & Friederici, 2002) and simulated using our forward model. In each plot, the solid line represents the ERP time course for the baseline condition while the dotted line represents the ERP time course for the experimental condition. The leftmost column gives the experimental condition associated with the row as well as the ERP component associated with such condition. For the empirical data, we selected the recordings at the most significant electrodes. For Synthetic ERP, the "most significant electrodes" are defined as the ones where the maximum peak amplitudes for a given component are simulated.

scalp measurements are ill-posed, the forward approach requires a model that makes precise what brain areas generate the component. As we shall now discuss, the participation of such areas can be segregated into two contributions: the source dipole orientation constrained by the gray matter surface and the pattern of activation.

6.1. Source dipole modeling and cortical geometry

We associated the cortical regions defined in the 2002 model to source dipoles by first mapping them onto our realistic brain mesh, and then averaging the normals to the surfaces of these areas to generate a representative dipole orientation. An important challenge concerned the 2002 model's use of multiple ontologies to define neural substrates of cognitive processes and ERP components. Functional regions were used alongside cytoarchitectonically defined Brodmann areas and coarse gyral ontologies. Since the critical factor for modeling the source of the electromagnetic field is the geometry of the gray matter surface, functional regions or Brodmann areas need to be converted to their associated gray matter surface location since only then can the orientation of the area's surface be retrieved. Moreover, the orientation may vary across a region, indicating the challenge of linking functioning neural circuitry to subregions or even voxels within a given region. We used the Destrieux atlas as a unified ontology providing the correct amount of detail to recast the mixed ontology of the 2002 model into a single brain atlas — an approach which highlights the lack of unified standards for delineating brain regions (and subregions).

As has been discussed previously in Section 1.3, the ill-posed nature of the electromagnetic inverse problem means that no unique source model can be obtained without the use of fallible a priori constraints. Accordingly, this approach can only provide a general localization of neural activity, such as the 2002 model's claim that a contributing source for the N400 resides in BA 45. As shown by Synthetic ERP simulations in Fig. 10, such limitations do not allow for faithful simulation of the canonical N400 scalp distribution (among others). Two solutions can palliate these limitations. The first one consists in finding within these areas the cortical patch providing the best fitting solution. If in the present paper we simply hand picked a better fitting dipole, future work could investigate the possibility of using the apparatus involved

in computing the inverse solution while constraining the search space to the source dipoles (or combination of source dipoles) associated with a given brain are. An example of a related approach to EEG source reconstruction including anatomical constraints on their solution space is given by Phillips et al. (2002). Another option would be to make direct use of the coordinates where fMRI revealed a significant increase of BOLD signal and posit this as the location of the relevant dipole. However, we have stressed that detailed processing models will in general show that a given epoch of processing for a given language subfunction involve the competition and cooperation multiple neural circuits beyond those restricted to areas of most significant BOLD activity — and this observation motivates our work on both Synthetic fMRI and Synthetic ERP, with the long-term goal of developing "doubly causal" models (more in Section 7) that can predict both fMRI and ERP signals under varied task conditions.

6.2. Activation modeling

We provided a way to use ERP data as a basis for modeling the time course of activations in brain areas that goes beyond a simple modeling of activation as a boxcar function defined on a period directly mapped in onset and offset time of an ERP component defined by some form of anomalous input. Our attempt to simulate the ELAN, N400, and P600 ERP components reported by Hahne and Friederici (2002) provided new insights into the challenges of relating neurolinguistic data and models to empirical ERP data through synthetic brain imaging. Nonetheless, this does not obviate the need for detailed processing models (Synthetic ERP Phase 1; see Section 7).

6.3. Quantitative ERP data extraction from literature

We have laid bare the difficulty of extracting quantitative ERP data from the literature in a format suitable for Synthetic ERP computational modeling. The appropriate data format needs to include the shape of the component or EEG trace measured under a variety of experimental conditions. Our ELAN simulation showed not only that a computational model should replicate the negative going component at around 100 ms but also the negative-going trend all through the epoch time. The common methodology of describing a component at the locus of electrodes as opposed to their average over larger scalp region also poses problem, as the electrode level precision seems too small a scale for Synthetic ERP. It also poses problems for the definition of ERP components themselves since a "most significant" electrode location cannot be empirically assigned to a component across subjects and experimental designs. Finally, the N400 simulation highlights the difficulty of clearly defining an ERP component when its particular field contribution is superimposed upon those from other concurrent processes, or when the component is known to have several functionally and scalp-voltage topographically distinct subcomponents as in the case of N100 or N400. We anticipate such superimposition of fields and diversity of subcomponents to be the norm for any sufficiently detailed description of neuroelectromagnetic dynamics associated with cognitive processing, and therefore recognize that qualitative accounts of ERP data are the limiting factor for any modeling or comparative exercise. In particular, we stress that many different neural processes may underlie a negativity occurring in a range around 400 ms, and so we may expect progress in neurolinguistics to depend strongly on the ability to discriminate different "N400s" rather than speaking of "the" N400.

7. A prospectus for Phase 1: From neural and schema networks to dipoles

Our long-term goal is to generate models with hypothesized circuitry localized to specific brain regions but competing and cooperating to yield overall behavior, making explicit how prior processing creates states that affect computing in the current epoch. The task is immensely simplified if it can be argued that the human circuitry for the function is a variation on circuitry in the monkey brain for which neurophysiological data are available. This was the case in studies of reach to grasp behavior (Arbib et al., 2003; Grafton, Fagg, & Arbib, 1998) and basic forms of working memory and auditory object processing (Deco, Rolls, & Horwitz, 2004; Husain et al., 2004; Tagamets & Horwitz, 1998, 2000). In these cases, Synthetic Brain Imaging was applied to predict synaptic activity in circuitry localized in different brain regions as the basis for computing predictions testable by PET or fMRI imaging. But what of ERP data? As indicated above, the strategy is to use computational models to predict the time course $d_A(t)$ of current equivalent dipoles for relevant areas of the brain, and then use forward modeling to derive predictions of ERP measurements. Unlike previous work on Synthetic Brain Imaging, model neurons must now be linked to cortical geometry so that dipole orientation can be defined in an anatomically sound fashion. We will show that neural network models of language processing seldom link circuits to brain regions, and then introduce our recent work employing interacting schemas to model language production and comprehension, while noting that it too has yet to be strongly linked to neurobiological data.

7.1. Testing a neural network model against ERP data using a forward approach: Modeling requirements

The goal of computational neurolinguistics is to build models that not only simulate a linguistic task or behavior (such as decomposing the sound wave of a word into phonemes, assigning the proper syntactic structure to a sequence such words, describing a visual scene, etc.), but also replicates underlying brain processes. Our discussion of the forward model part of Synthetic ERP (Phase 2) showed that ERPs imposes important requirements on neural network modeling. Table 3 offers a preliminary presentation of these requirements for various features of neural network models. Such requirements will be at the heart of the future work on Phase 1 of Synthetic ERP.

7.1.1. The minimal neuron model for combining Synthetic Brain Imaging and Synthetic ERP

For Synthetic Brain Imaging, we require the time course of synaptic activity for all neurons in each simulated brain region. This can then be passed through the hemodynamic function and averaged appropriately to yield predictions for PET or fMRI. However, although the model may contain many neurons in both cortical and non-cortical regions, the neurons most relevant to the ERP signal are cortical pyramidal cells and the most relevant aspect of their activity is the PSPs in their apical dendrites. Moreover, the contribution of these dendrites to the dipoles integrated into $d_A(t)$ for a specified region A depend crucially on their orientation. Thus, whereas the modeling of neurons for Synthetic Brain Imaging can ignore the spatial location of its constituent neurons, modeling of the cortical pyramidal cells for Synthetic ERP must represent not only the location but also the orientation of the neurons. We stress that in general the model will include other cell types from cerebral cortex as well as circuitry in subcortical regions — but the activity of these cells is not included in Phase 2 of Synthetic ERP. In our discussion of forward modeling, we introduced a head model which represents the surface of cerebral cortex by a mesh (see 4.2, details in Appendix C). Hence, in a computational model of cortical processing to be used with Synthetic ERP, the location of all pyramidal cells must be specified either (a) as being below a specific face of the mesh or (b) below some larger "slab" obtained by aggregating a number of contiguous faces and assigning them

Table 3
Preliminary *requirements* imposed on computational neural networks by *constraints* associated with the use of an EEG forward model. For each feature of a neural network model outlined in the leftmost column, the central column stipulates the new constraints imposed on this feature by the use of the Synthetic ERP phase 2 forward model. The rightmost column converts these constraints into requirements that the feature needs to meet in order to be used in Synthetic ERP. Although we have exemplified Synthetic ERP with examples from computational neurolinguistics, this table offers guidelines of more general applicability. In particular, they should help orient neural network modeling for both systems and cognitive neuroscience towards model types that facilitate contact with ERP data.

Model features	Constraints	Requirements
Neuron model	- Current dipole's amplitude is linked to synaptic activity - Neural activity should be simulated with a ms precision	- Allow the quantification of synaptic activity - Account for the impact of synaptic activity characteristic times on processing times
Neuron types	Only the synaptic activity of pyramidal cells contributes to EEG signal	For Phase 1, the model must include all cell types required to provide circuitry that performs the stated tasks and can be tested against single-cell data (where applicable). For the current version of Phase 2, anatomical localization and orientation must be defined for the cortical pyramidal cells included in the model
Brain area model	The cortical geometry is a key parameter of ERP modeling	Map each neural layer representing a given brain region onto a 3D mesh model of the cortical surface geometry using an existing surface atlas. Neurons in a layer should carry hypotheses on their cell type and connectivity but also on their 3D location on the cortical surface
Overall network architecture	Signal conduction times between brain regions need to be accounted for	- Incorporate into the large-scale connectivity between neural layers the known white matter connectivity between the brain regions they represent - Account for the action potential propagation delays in the white matter tracks

an averaged orientation. Each cell is then oriented orthogonally to the face or slab to which it is assigned, and we must then employ a neural model that yields the time course of PSPs of the apical dendrites. Given the resulting spatial structure and the fine temporal resolution required to compute the ERP, we need to include axonal propagation time in the model, and for this reason it would seem that spiking models would serve better than rate models. The simulated PSPs of apical dendrites would provide the 3D distribution of dipoles, fixed in orientation but time-varying in amplitude, to drive the forward model. The result would be the Synthetic ERP for the phenomenon captured by the simulated network.

7.1.2. Cortical geometry and surface atlases

Synthetic ERP is not alone in stressing the importance of cortical geometry in defining the position and orientation of EEG sources (see Table 1). However, our approach to the forward problem both within the framework of neurolinguistics and as a tool to move from conceptual to computational models lead us to reposition this issue at the center of the forward problem. The analysis of the current dipole model and of the head model (see 4.2 and Appendix B), as well as the problems raised by the mapping of the brain regions defined by the 2002 model onto a single surface atlas (see 5.1) show the issue of cortical geometry to be much richer than that of merely constraining dipole orientation as normal to the cortical surface.

In order to quantitatively account within a computational framework for the impact of cortical folds on the EEG signals, we suggest the following questions be addressed within models of cerebral cortex:

(1) How to quantitatively constrain the electric sources orientation and position by the geometry of the cortical surface?
(2) What cortical surface should be used? Individual cortical surfaces or population-average templates?
(3) What surface atlas should be used to parcellate the cortical surface and ensure a standard mapping between the brains of various individuals?

Question (1) is commonly addressed in the forward modeling literature through the use of 3D meshes representing the cortical surface. A dipole can then be constrained in orientation by the normal vector of a given face of the mesh. Its impact on neural network modeling has been detailed in the preceding section (see 7.1.1).

Question (2) raises the issue of the type of cortical surface used. The lack of inter-individual correspondence in cortical folding makes any attempt to define population-average templates difficult. The well-documented case of the duplication of Heschl's gyrus in some individual (two gyri instead of one) provides a good example (Leonard, Puranik, Kuldau, & Lombardino, 1998). Heschl's gyrus is part of the primary auditory cortex which, according to the 2002 model, performs acoustic analysis and phoneme identification, linked to the N100 ERP component. How should these variations in Heschl's gyrus' morphology be incorporated in the framework of computational modeling? How do they impact the forward modeling of N100? In part, the answer may well depend on the precision with which the ERP data are presented. If the data average over a number of subjects without separation with respect to, at least, gross differences in gyrification, then it may be appropriate to use the simpler anatomy as the basis for Synthetic ERP modeling.

Specifically, our simulations are based on a cortical mesh generated from high resolution MRI scans for a single individual (MNI Colin 27, see Appendix C). However, the fact that ERPs are usually reported in the literature as population averages begs the question of whether the use of a population-average template would not be more appropriate. Most of the existing EEG source localization software (e.g. Oostenveld et al., 2011; Tadel, Baillet, Mosher, Pantazis, & Leahy, 2011) address this issue by offering the possibility to either (a) use a cortical mesh extracted from an anatomical MRI scan of the individual from whom the EEG signal has been recorded or (b) use a standard brain mesh (such as MNI Colin 27) that can be warped to match sensors locations or be used with standard sensor locations (which is similar to our choice). However, (a) seems unsatisfactory for computational neurolinguistics since most ERP data reported in the literature do not come with associated cortical meshes. As to (b), the possibility to use a population-template brain mesh is undermined by fact that averaging surfaces from different brains remains a challenge for which no standard solution has yet emerged (Auzias, Colliot, Glaunes, Perrot, & Mangin, 2011; Dale, Fischl, & Sereno, 1999; Fischl, Sereno, & Dale, 1999; Lyttelton, Boucher, Robbins, & Evans, 2007; Van Essen, 2005). Moreover, such an average seems more likely to blur gyrification rather than provide a useful standard. Thus, for now, it seems a reasonable strategy to use MNI Colin 27 as the basis for localization and orientation of cortical areas for a neural network model.

Question (3) emphasizes the issues raised by the diversity of brain region atlases used by modelers, the difficulty to quantitatively define the relations between them, and the difficulty to link some of them to cortical geometry. The 2002 model offered a good example of this, using of a mixed ontology including parcellations

of the cortical surface based on neural cytoarchitecture (Brodmann areas), cortical folds (gyri and sulci), function (e.g. auditory cortex), and lesion data (e.g. Broca's area) (see Table 2). Without quantitative treatment of these various nomenclatures, all pose problems for the simulation of EEG signals. Individual variation in cortical folds was already mentioned in relation to point (2), but in addition the idiosyncratic variations of localization within the cortical folds of Brodmann areas have only recently started to be quantitatively analyzed (Fischl et al., 2008). In particular, linking computational neurolinguistic models to ERP data will require a deeper analysis of recent findings on the individual variations in Broca's area anatomy (Keller et al., 2009).

Finally, we note that the incorporation of empirical data from non-human primate studies into neurolinguistic modeling, such as single cell recordings or white matter connectivity, raises between-species homology challenges (Arbib & Bota, 2003; Deacon, 2004). Neural networks have been extensively used to model the brain functions of non-human primates. Their use in neurolinguistics should be thought of not only in terms of their computational power, but also as a way to make contact with computational models of results from monkey neurophysiology. This approach will incorporate evolutionary hypotheses into neurolinguistic computational models and test them against human neuroimaging data.

7.2. Models of language processing

The vast majority of neural network models associated with language processing are unconstrained by brain imaging or ERP data. A number of interesting models have, for example, used Simple Recurrent Networks which can be trained, e.g., to learn sequences in a way which replicates application of simple constructions in forming sentences. Among the deepest studies of this kind is one that addresses a range of psychological and developmental data (Chang, 2002; Chang, Dell, & Bock, 2006) but it does not address neurophysiological or neurological data. Another model only addresses lexical access but does offer some insight into aphasia (Dell, Schwartz, Martin, Saffran, & Gagnon, 1997). The GODIVA model of sequencing phonemes to form words (Bohland, Bullock, & Guenther, 2010) does address a range of neurophysiological data but is clearly at a lower level of language processing than those that have engaged us in this article. Dominey, extending earlier research modeling linkages between cortex, basal ganglia and brain stem in the control and learning of eye movements (Dominey & Arbib, 1992; Dominey et al., 1995), provides a neurally plausible model of the interaction of syntax and semantics in the parsing of very simple sentences (Dominey, Hoen, & Inui, 2006; Dominey, Inui, & Hoen, 2009). The model employs recognition of the sequence of function words in a sentence to provide access to the syntactic construction that assigns the content words to their semantic roles. Previous attempts at relating artificial neural network activity to language-related ERPs include models of the dynamics of neural masses (David et al., 2011; Yvert et al., 2012) but do not simulate the information processing whereby the brain performs a given linguistic task (recall Table 1). Another approach employs simple Hebbian networks but does not analyze the impact and role of forward models on ERP signal simulation (Garagnani, Wennekers, & Pulvermüller, 2008).

Of course, a major obstacle to neurophysiologically realistic models of language processing is that only humans possess language in the sense of an open-ended lexicon and a grammar that allows the flexible production and comprehension of utterances that convey novel meanings in diverse domains of discourse. As noted earlier, there are two strategies for development of fine-scale models of language processing that follow from this:

(1) One is to employ evolutionary hypotheses to create models that combine (i) modules whose detailed neural circuitry can be related to that of non-humans executing a *similar* subfunction and (ii) modules executing *human-specific* subfunctions for which the circuitry can be structured on the basis of the evolutionary hypotheses (see Aboitiz, 2012; Aboitiz, Aboitiz, & García, 2010; Arbib, 2006, 2010, 2012, for examples of such hypotheses).

(2) The other is to abandon the use of simulated neurons as the unit of processing and instead use networks of interacting schema instances to work at a scale slightly coarser than that of neurons, but far more detailed than that of brain regions. Schema theory has been employed successfully over the years in modeling visually guided behaviors in frogs, rats, monkeys and humans where we make crucial hypotheses as to the localization of schemas in different parts of the brain. It was introduced to neurolinguistics by Arbib and Caplan (1979); and we further developed links between schema theory and language (aphasia, acquisition, production) in Arbib, Conklin, and Hill (1987). Most recently, we have extended schema theory to define Template Construction Grammar as a mechanism linking vision and language in the description of visual scenes (Arbib & Lee, 2007, 2008), but this model includes no hypotheses on cerebral localization of schemas (though Lee and Barrès (2013) have taken a small step in this direction by discussing some aspects of aphasia). However, this article is not the place to present background and references on schema theory, but only to introduce the gap that currently exists between schema theory and the constraints of Synthetic ERP. Crucially, schema-theoretic models in their current form cannot support Synthetic ERP for at least two reasons:

(a) Spatial: To employ Synthetic ERP, various schema subnetworks would have to be assigned to different faces or slabs of a cortical mesh or linked to subcortical regions;
(b) Temporal: To compute $d_A(t)$, "schema time" would have to be mapped onto "neural time", and competition and cooperation between cortical schema instances would have to be mapped to patterns of activation of apical dendrite PSPs.

Solving (a) lies within the remit we have established within this article for neural network modeling, whereas (b) poses new challenges — but challenges that must be met since schema theory serves as a bridge between the language of psychology and the language of neuroscience, and this "translation" needs to be extended to link ERPs as a tool for psycholinguistic observation to a deeper understanding of the patterns of information processing distributed across the brain.

Nonetheless, some links and challenges for the spatial problem can now be made explicit. A phoneme recognition schema could be relatively well localized around Heschl's gyrus. However, semantic memory can be represented as a widely distributed schema network, making explicit the problem of mapping onto the cortical geometry required for ERP modeling. There do exist a range of conceptual models which complement the 2002 model by offering competing views of how to systematize imaging and ERP data by localizing different processes in different parts of the brain, but they lack computational specificity (e.g. Hagoort, 2005; Hickok, 2009). Schema theory however offers the flexibility to vary the levels of detail incorporated in a brain model depending on the current state of knowledge while maintaining brain-oriented computational principles at all levels. Its role is to ensure that at each stage of our understanding of a brain function, we can express our knowledge in a computational form that can provide simulation results that stimulate further research, both empirical and computational. Each schema can then be broken down into further sub-schemas (and, potentially, down to biologically grounded neural networks) once the brain processes it represents are better understood.

7.3. In conclusion

Our earlier work on Synthetic Brain Imaging was motivated by the need to link neural models (inspired in part by data from primate neurophysiology) to the results of human brain imaging. The present work addresses the challenge of linking such models to ERP data (and, although we have not discussed it here, the data of magnetoencephalography). We saw that whereas DCM addresses the issue "What aggregated measures of underlying neural activity could cause the observed ERP recordings?" our new Synthetic ERP methodology is doubly causal, based on two phases:

Phase 1 addresses the question "What patterns of interaction in neural circuitry could cause the observed behavior (and explain single-cell recordings, where available)?" whereas

Phase 2 addresses the question "Could the aggregate activity of neurons in the circuitry so modeled cause the observed ERP recordings?"

We have seen that Phase 2 is well-defined and has much in common with DCM, but enforces the assumption that ERPs be calculated using a forward model on the basis of dipoles whose orientation is provided by orientation of the corresponding region of cortex, rather than having arbitrary orientations based on one of the many possible solutions to the inverse problem posed by observed ERP data.

However, our work on Phase 1 is at an earlier stage of development. The key point is that, in addition to the requirements of neural network models used for Synthetic Brain Imaging that they can be tested against single-cell data (where available) as well as behavioral data, the neural networks used for Synthetic ERP must include neuroanatomically realistic placement and orientation of cortical pyramidal neurons. However, work on Phase 1 cannot (in general) succeed if only cortical regions are modeled — subcortical structures such as basal ganglia and thalamus may play a crucial role.

All this poses exciting challenges for future work in *neural networks* that is intended to contribute to computational modeling for systems and cognitive neuroscience. In particular, future work in neurolinguistics will depend on both new approaches to the structuring of empirical data and on the development of novel computational models of language processing.

Finally, we noted the power of schema network models in explaining behaviors for which the pool of relevant neuron-level data is impoverished, but then raised the daunting question of how to link activity of schema networks to anatomically localized and oriented dipoles, in both space and time.

Acknowledgments

This material is based upon work supported in part by the National Science Foundation under Grant No. 0924674 (Michael A. Arbib, Principal Investigator). Our thanks to Ambuja Tiruvoimozhi for valuable discussions of techniques and toolboxes for forward modeling.

Appendix A. General physical formulation of the forward problem

Solving the forward model for EEG recording consists in determining the electrical field generated by neural current sources and measured by electrodes on the scalp. The 4 Maxwell equations give the most general expression of the problem. Given the relatively slow changes of the electric and magnetic fields generated by neural sources (below 100 Hz), we can use the quasi-static approximation of Maxwell's equations:

$$\begin{cases} \nabla \cdot E = \dfrac{\rho}{\varepsilon\varepsilon_0} \\ \nabla \cdot B = 0 \\ \nabla \times E = 0 \\ \nabla \times B = \mu_0 J \end{cases} \tag{A.1}$$

as well as

$$\nabla \cdot J = 0 \quad \text{(Conservation of charge)}, \tag{A.2}$$

where E is the electric field, B the magnetic field, J the current density, ε the permittivity of the milieu, ρ the charge density, and μ_0, ε_0 are respectively the permeability and permittivity of free space.

It is convenient to separate the primary currents J^P, which correspond to the currents generated directly by the neural sources and creating the electric field, from the secondary or return currents J^S which are caused by the existence of the field. Following Ohms law we write $J^S = \sigma E$, where σ is the conductivity (which need not be isotropic or homogeneous in the general case). It follows that:

$$J = J^P + \sigma E. \tag{A.3}$$

Finally, since E is irrotational, we can define a scalar potential V such that:

$$E = -\nabla V. \tag{A.4}$$

From there the *Poisson equation for the electric potential*:

$$\nabla \cdot (\sigma \nabla \mathrm{V}) = \nabla \cdot J^P. \tag{A.5}$$

We are interested in the potential only at the positions on the scalp where electrodes are located. Solving the forward problem for EEG consists in solving the Poisson equation for primary currents generated by the brain's activity. To do so, one needs to stipulate: (a) what the primary current sources are: this is the role of the *current dipole model* (see Appendix B); (b) what the conductivities are: this is the role of the *head model* (see Appendix C); a method (analytic or numerical) to solve the Poisson equation: we review here the *Boundary Element Method* (BEM) (see Appendix E).

Appendix B. Dipole modeling of current sources

Although the activity of every neuron generates currents, both in the dendrites and in the axons, the activity of individual neurons is not sufficient to yield a detectable electric field at the surface of the scalp. Only the local summation of the currents generated by many neurons can result in measurable changes in the electroencephalogram. For currents to be additive, neurons need to be synchronously active and have a spatial arrangement that enables the amplification of the field. Such a configuration is found in the *pyramidal neurons* of the cortex whose dendritic currents are thought to be the main sources of EEG signals. Neighboring pyramidal neurons have apical dendrites arranged parallel to one another and perpendicular to the cortical surface in a palisade-like configuration (cf. Fig. 14, left). Dendrites and not axons can display significant synchronous activity since the duration of post synaptic potentials is much longer than that of action potentials, favoring overlapping activation between cells. Finally the excitatory synapses tend to be localized at the apex of the dendritic tree of pyramidal neurons, while the inhibitory synapses tend to cluster around the soma.

Focusing on excitatory synapses, excitatory post-synaptic potentials (EPSPs) result in the pyramidal neurons in currents flowing both in the dendrites and in the extra-cellular environment

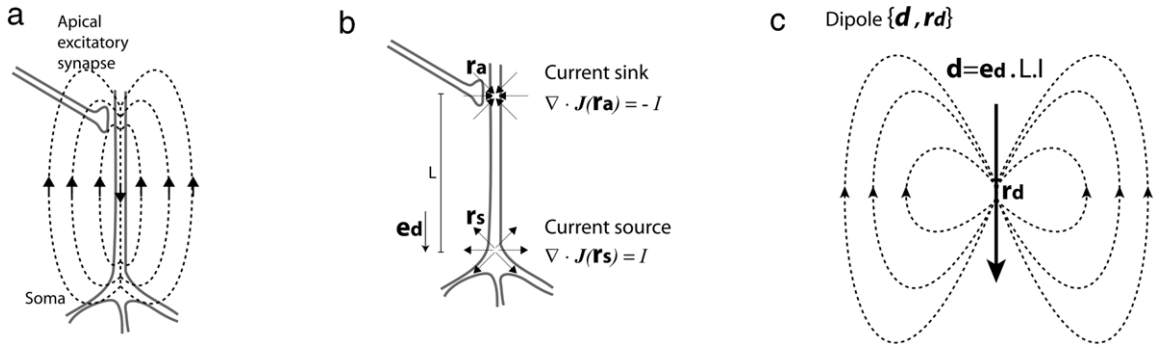

Fig. 13. Modeling of a pyramidal neuron as a current dipole. (a) Currents generated by an apical excitatory synapse in the pyramidal neuron. Excitatory synapses tend to be localized in the apical region of the dendritic tree of pyramidal neurons, while inhibitory synapses tend to be localized near the soma. Currents are generated both in the dendrite and in the extracellular environment. (b) Model of the same neuron as a current sink and a current source located at the apex and at the soma of the neuron respectively. The source and sink are modeled as punctual, separated by a distance L, and "pumping" an equivalent amount of current I. (c) Such a configuration can be modeled as a current dipole oriented from the sink to the source, located between the two sources, and whose moment is equal to the product of the current "pumped" by the distance between sources. Such a dipole approximation is valid when the distance at which the field is measured is large compared to L.

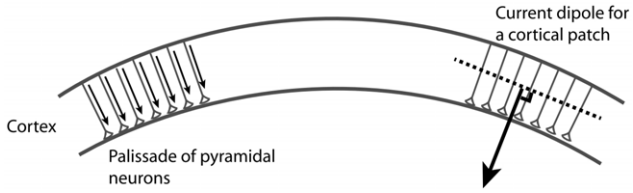

Fig. 14. Mesoscopic current dipole model of a patch of cortex. On the right side is depicted the unique organization of pyramidal cells in a palisade-like layer in which the apical dendrites are all oriented perpendicular to the cortical surface. Each neuron is here modeled as a current dipole (cf. Fig. 13). On the left side, the whole patch of cortex is modeled as a unique dipole representing the summed contributions of each individual neuron. This summation is made possible by the configuration of apical dendrites. The resulting dipole is perpendicular to the cortical surface and located at the center of the cortical patch. Such a mesoscopic dipole model rests on the hypothesis that any deviation from collinearity of neuron-level dipoles is small (i.e. curvature of cortex is negligible), the distance between neuron-level dipoles is small compared to the distance between the cortical patch and the locus of measurement of the field, and finally that the neurons' activities coincide at least partially in time. This possibility to sum up individual neuron current contributions is a necessary condition for a current source to be strong enough to yield an electric field that can be measured using EEG.

that can be modeled as in Fig. 13(a). In turn, such currents can be modeled as a current sink at the apex and a current source at the soma, equal in strength, separated by a distance L. Fig. 13(b) represents such a model with r_a the position of the apical sink, r_s the position of the source at the soma, J the current density, and e_d a unit vector pointing from the sink to the source. This configuration can further be modeled as current dipole $\{d, r_d\}$ as presented in Fig. 13(c). The dipole is assigned to the position $r_d = \frac{r_s+r_a}{2}$. Its moment is defined as $\|d\| = d = L \cdot I$. The dipole is oriented along e_d from the sink to the source.

Modeling of a current sink and source equal in strength by a dipole can be derived from the multipole expansion of the formulation of the field. In this formulation, the first order dipole approximate of the source gives a good account of the field when the distance at which the field is measured is large compared to L. A current dipole can therefore be used at a microscopic level to model the electric activity of a single pyramidal cell.

On the left of Fig. 14, is schematized a layer of pyramidal neurons, each one associated with a current dipole. The specific spatial configuration results in all the neuron-level dipoles to be oriented perpendicular to the cortical surface. To the extent that the curvature of the cortex can be neglected, the dipoles can be approximated as locally collinear.

As shown in Fig. 14 (right), a patch of cortex can therefore be represented by a mesoscopic-level dipole summarizing the activity of the pyramidal neurons. However, such an extra step in modeling the current sources is valid only inasmuch as: (1) the deviation from collinearity in the dipoles due to cortical curvature is negligible, (2) the neuron-level dipoles are close to each other relative to the distance of measurement of the field, and (3) the activity of the neurons is hypothesized to be synchronous. Given these hypotheses, a current dipole can be used to model the dendritic currents generated by a population of pyramidal cells in a small patch of cortex. The 6 parameters that define the dipole can in theory be specified: it is located at the center of the patch, oriented perpendicular to the cortical surface pointing inward, its amplitude can be derived from the synaptic activity of the given neuronal population.

Primary current sources can from here be modeled either as *focal single dipoles* (in the case of a few very local activations, a common hypothesis for modeling epileptic seizures), or as *dipoles distributions* (in which case large patches of cortex are modeled as a distribution of dipoles anatomically constrained by the cortical topology).

Appendix C. Conductor modeling: the head model

Solving Eq. (A.5) requires not only the definition of the primary sources (see Appendix B) but also the definition of the conductivity tensor $\sigma\left(\overrightarrow{r}\right)$ of the media in which the electric field propagates. To do so we make the following hypotheses: (1) the head as a conductor can be modeled as a series of embedded conduction volumes, typically brain, skull, and scalp (but more complex models can be considered); (2) the boundary between these volumes can be modeled by realistic meshes extracted from anatomical MRI (spherical head models can also be used that allow analytical solutions); (3) the conductivity of each conduction volume can be considered homogeneous and isotropic.

The last point allows the use of the Boundary Element Method to find numerical solutions to Eq. (A.5) (see Appendix E). However, the isotropy hypothesis has been challenged in the case of the skull and white matter. In addition, the values of the conductivities are still debated and tend to depend on the method used to measure them (for a review see Hallez et al., 2007).

Fig. 15 describes the head model we used in our work. The absence of a model of subcortical elements is a limitation of most head models. In addition, the use of a head model in the computation of EEG signals begs the question of "what head" should be used. We here use a realistic head model derived from high-resolution anatomical MRI data acquired from a single subject. But no standard has so far been developed for the head model.

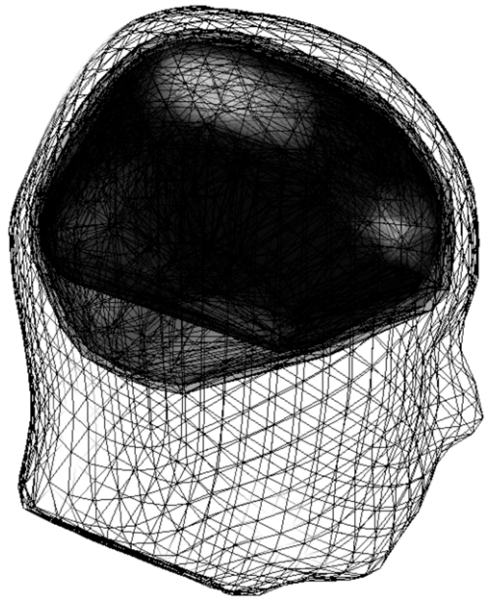

Fig. 15. The head model. The head model defines the media in which the electric field propagates. We use a realistic head model composed of 4 conduction volumes. From the innermost volume to the outermost: brain, cerebrospinal fluid, skull, and scalp. These volumes are separated by boundaries defined as triangular meshes: gray matter surface, inner skull, outer skull, and scalp. The meshes are computed from 27 high-resolution anatomical MRI images of a single individual (MNI meshes provided by Brainstorm and extracted using BrainVisa software). Except for the scalp mesh, we used the convex hull associated with the MNI Colin27 meshes to alleviate computation. In our work, we make the hypothesis that each volume has a homogeneous and isotropic conductivity.

The implementation of Phase 2 of Synthetic ERP reported here uses a 4-compartment head model based on the MNI Colin27 MRI scans (Evans et al., 1993; Mazziotta et al., 1995) which provides meshes respectively representing the surfaces defined by the gray matter, the inner skull, the outer skull, and the outer surface of the scalp. The ventricles are ignored in the present model. The meshes are triangular meshes provided by the Brainstorm default anatomy (Tadel et al., 2011) and extracted from the MNI Collins MRI scans using BrainVisa software. If the exact geometry of the brain surface is required to compute the orientation of the dipoles, the computation of the electromagnetic field can be greatly alleviated with a minimal impact on the solution by simplifying the geometry of the conduction volumes. For this reason, the head meshes which define the volume boundaries of the head model for the computation of the forward solution are the convex hulls associated with the MNI Colin27 brain, inner skull, and outer skull (but the scalp mesh was kept in its Brainstorm version for display purposes). We used the conductivity measurements provided by Oostendorp et al. (2000) (Brain: 0.22, CSF: 1.79, Skull: 0.015, Scalp: 0.22 S/m).

Few ERP experiments report the stereotactic positions of the electrodes used during the EEG recording. Synthetic ERP therefore uses default 65 electrodes 10/10 standard electrode systems and electrodes positions provided by Brainstorm (for a review of the existing electrode systems see Jurcak, Tsuzuki, and Dan (2007)). (See Fig. 16.)

Appendix D. Algebraic formulation

For multiple points of measurements of the electric potential (electrodes) and multiple sources (dipoles), it is useful to give the forward problem a compact algebraic formulation. Given a dipole with position r_{dip} and moment d, the electric potential measured at an electrode with position r solution of the Poisson equation (6) can be written:

$$V(r) = g(r, r_{dip}, d). \tag{D.1}$$

The Poisson equation is linear. If we note $d = d.e_{dip}$, where $\|e_{dip}\| = 1$, we can write:

$$V(r) = g\left(r, r_{dip}, e_{dip}\right) \cdot d. \tag{D.2}$$

The electric potential generated by a dipole at the location of an electrode depends linearly on the amplitude of the dipole, i.e. on the neural activity. However, it does not depend linearly on the position and orientation of the dipole (defined by the geometry of the cortex).

For **N dipoles** $\left\{r^j_{dip}, e^j_{dip}, d^j\right\}$, $j \in [\![1, N]\!]$, and **K electrodes** with positions r^k, $k \in [\![1, K]\!]$, given the linearity of the Poisson equation, we can write:

$$\forall\, k \in [\![1, K]\!], \quad V\left(r^k\right) = \sum_{j=1}^{N} g\left(r^j, r^j_{dip}, e^j_{dip}\right) \cdot d^j. \tag{D.3}$$

Therefore:

$$V = GD, \tag{D.4}$$

with:

$$V = \begin{bmatrix} V\left(r^1\right) \\ \cdots \\ V\left(r^K\right) \end{bmatrix} \in \mathbb{R}^K,$$

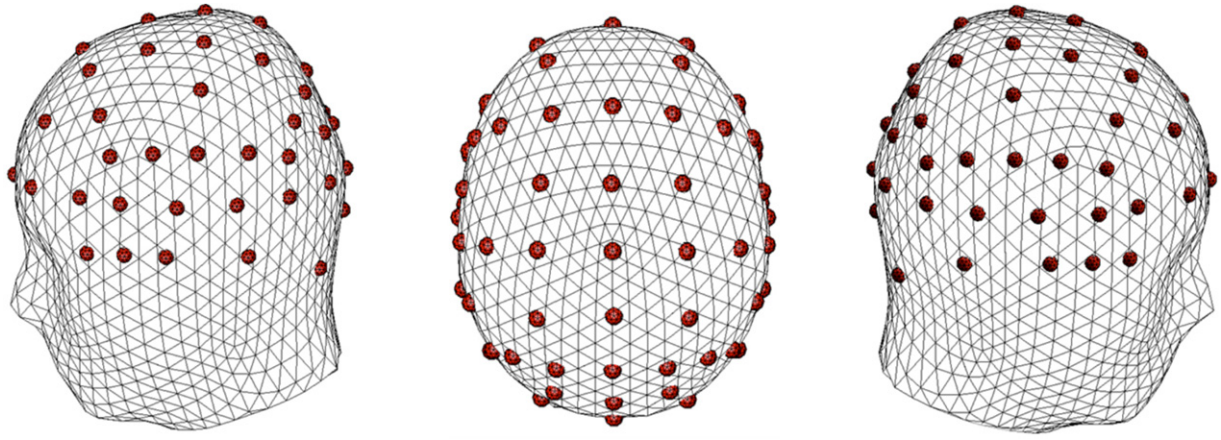

Fig. 16. Sensors positions. Sensor positions are defined as the default MNI coordinates of the 10/10 65 channels EEG electrode cap as defined by Brainstorm and associated with the MNI Collins head meshes. The electric field, output of the forward model, is computed at the sensors' positions.

electrode measurements vector, function of the electrodes positions.

$$G = \begin{bmatrix} g\left(r^1, r^1_{dip}, e^1_{dip}\right) & \cdots & g\left(r^1, r^N_{dip}, e^N_{dip}\right) \\ \cdots & \ddots & \cdots \\ g\left(r^K, r^1_{dip}, e^1_{dip}\right) & \cdots & g\left(r^K, r^N_{dip}, e^N_{dip}\right) \end{bmatrix} \mathbb{R}^{K\times N},$$

gain matrix function of the sources positions, orientations, and of the electrodes positions.

$$D = \begin{bmatrix} d^1 \\ \cdots \\ d^N \end{bmatrix} \in \mathbb{R}^N,$$

dipole amplitudes vector.

If the positions of electrodes are fixed as well as the position and orientation of the sources with only the amplitudes of the sources varying in time, Eq. (D.4) can be rewritten

$$V(t) = GD(t). \tag{D.4′}$$

Since the gain matrix G does not depend on time in these conditions, it can be computed only once for a set of sources. The EEG recordings $V(t)$ is simply a linear combination of the *source waveform functions* $d^j(t)$, $j \in [\![1, N]\!]$.

Appendix E. Numerical method: boundary element method (BEM)

Although analytical solutions can be found for the Poisson equation (see Appendix A, Eq. (A.5)) in the case of spherical head models, the use of realistic head models requires the use of numerical methods. In the case of homogeneous and isotropic conductivities, which remains a common assumption for the forward problem, Eq. (A.5) can be numerically solved using the Boundary Element Method (BEM). In more complex cases (conductivities non-isotropic and/or non-homogeneous), other methods are available such as Finite Element Method (FEM). The strength of the BEM rests in the fact that the potential at any point on a boundary can be determined by its values on the other boundaries. Hence only these boundary values needs to be numerically computed which reduces the size of the problem. Since for EEG we are measuring the electric potential on the scalp, we are only interested in the values on this boundary. FEM approaches on the other hand require computing numerical values for the electric potential at every point in space. In a nutshell, the BEM approach consists in computing the values of the electric potential on the conductors' volumes boundaries by approximating the continuous boundaries as a tessellation of small boundary elements.

The BEM rests on the integral formulation of the Poisson equation in the case of N_V conductor volumes of conductivities σ_k separated by N_S surface boundaries S_i. Due to the linearity of the problem (see preceding section), we will here, without loss of generality, consider the case of a single source dipole $\{r_{dip}, d\}$. It has been shown elsewhere (Sarvas, 1987) that the integral formulation of Eq. (A.5) can be written:

$$V(r) = \frac{2\sigma_0}{\sigma_k^- + \sigma_k^+} V_0(r) + \frac{1}{2\pi} \sum_{j=1}^{N_S} \frac{\sigma_j^- - \sigma_j^+}{\sigma_k^- + \sigma_k^+} \left(\oint_{r'\in S_j} \frac{V(r')}{\|r-r'\|^2} \frac{r-r'}{\|r-r'\|} dS_j \right), \quad \text{for } r \in S_k, \tag{E.1}$$

where V_0 is the potential that would be generated by the dipole source in an infinite medium whose conductivity is that of the medium in which the source is located (the brain in our case). σ_0 is the conductivity of this medium (here the conductivity of the brain). For a point $r \in S_n$, σ_n^+ and σ_n^- refer respectively to the conductivity outside and inside the boundary defined by S_n.

In the case of a current density distribution modeled as a single dipole $\{r_{dip}, d\}$, $V_0(r)$ has a straightforward analytical value:

$$V_0(r) = \frac{1}{4\pi\sigma_0} \frac{d\cdot\left(r - r_{dip}\right)}{\left\|r - r_{dip}\right\|^3}. \tag{E.2}$$

The boundary element method consists in first approximating the surface integrals in Eq. (E.1) by *tessellating each surface boundary* S_k into n_{S_k} triangles surface elements $\Delta_i^{S_k}$, $i \in [\![1, n_{S_k}]\!]$. Eq. (E.1) can then be approximated by:

$$V(r) = \frac{2\sigma_0}{\sigma_k^- + \sigma_k^+} V_0(r) + \frac{1}{2\pi} \sum_{j=1}^{N_S} \frac{\sigma_j^- - \sigma_j^+}{\sigma_k^- + \sigma_k^+} \times \sum_{i=1}^{n_{S_j}} \left(\int_{r'\in\Delta_i^{S_j}} \frac{V(r')}{\|r-r'\|^2} \frac{r-r'}{\|r-r'\|} dS_j \right). \tag{E.3}$$

The second step consists in approximating $V^j(r)$ on each boundary S_j by $\tilde{V}^j(r)$ defined as the linear combination of simple basis functions $h_p(r)$, $p \in [\![1, n_{S_j}]\!]$.

$$\tilde{V}^j(r) = \sum_{p=1}^{n_{S_j}} V_{j,p} h_p(r). \tag{E.4}$$

We can then rewrite Eq. (E.3):

$$V(r) = \frac{2\sigma_0}{\sigma_k^- + \sigma_k^+} V_0(r) + \frac{1}{2\pi} \sum_{j=1}^{N_S} \frac{\sigma_j^- - \sigma_j^+}{\sigma_k^- + \sigma_k^+} \times \sum_{i=1}^{n_{S_j}} \sum_{p=1}^{n_{S_j}} V_{j,p} \left(\int_{r'\in\Delta_i^{S_j}} \frac{h_p(r')}{\|r-r'\|^2} \frac{r-r'}{\|r-r'\|} dS_j \right). \tag{E.5}$$

A common choice for the basis function is to consider the set of basis functions such that on surface S_j

$$h_p(r) = \begin{cases} 1 & \text{if } r \in \Delta_p^{S_j} \\ 0 & \text{otherwise,} \end{cases}$$

which corresponds to an approximation that the electric potential is constant on each triangular boundary element.

The final approximation consists in defining so called *collocation points* at which the basis functions will be numerically estimated. The collocation points are typically the centroids of the triangular boundary elements.

Writing Eq. (E.5) for each one of these collocation points result in a set of equations that can be solved to determine the coefficient $V_{j,p}$ for each triangular element p on each surface S_j.

The forward problem corresponds in this case in solving a system of linear equations, which requires the inversion of a dense matrix with a size of the order of number of boundary elements defined. The size of the matrix is relatively small since we do not need to compute parameters for each point in the volume and depends on the coarseness of the tessellations used.

Going back to Eq. (D.4′) (see Appendix D), the matrix inversion need only to be done once for a given location and orientation of the dipole sources (and location of the sensors) to define the gain matrix.

In this paper, the forward model is computed using the FieldTrip (Oostenveld et al., 2011) MatLab implementation of OpenMEEG version of BEM (Gramfort et al., 2011).

References

Aboitiz, F. (2012). Gestures, vocalizations and memory in language origins. *Frontiers in Evolutionary Neuroscience*, *4*.

Aboitiz, F., Aboitiz, S., & García, R. R. (2010). The phonological loop: a key innovation in human evolution. *Current Anthropology*, *51*, S55–S65.

Aboitiz, F., Scheibel, A. B., Fisher, R. S., & Zaidel, E. (1992). Fiber composition of the human corpus callosum. *Brain Research*, *598*, 143–153.

Amunts, K., Lenzen, M., Friederici, A. D., Schleicher, A., Morosan, P., et al. (2010). Broca's region: novel organizational principles and multiple receptor mapping. *PLoS Biology*, *8*, e1000489–e89.

Amunts, K., & Zilles, K. (2012). Architecture and organizational principles of Broca's region. *Trends in Cognitive Sciences*, *16*, 418–426.

Arbib, M. A. (2006). Aphasia, apraxia and the evolution of the language-ready brain. *Aphasiology*, *20*, 1–30.

Arbib, M. A. (2010). Mirror system activity for action and language is embedded in the integration of dorsal and ventral pathways. *Brain and Language*, *112*, 12–24.

Arbib, M. A. (2012). *How the brain got language: the mirror system hypothesis*. New York & Oxford: Oxford University Press.

Arbib, M. A., Billard, A., Iacoboni, M., & Oztop, E. (2000). Synthetic brain imaging: grasping, mirror neurons and imitation. *Neural Networks*, *13*, 975–997.

Arbib, M. A., Bischoff, A., Fagg, A. H., & Grafton, S. T. (1995). Synthetic PET: analyzing large-scale properties of neural networks. *Human Brain Mapping*, *2*, 225–233.

Arbib, M. A, & Bota, M. (2003). Language evolution: neural homologies and neuroinformatics. *Neural Networks: The Official Journal of the International Neural Network Society*, *16*, 1237–1260.

Arbib, M. A., & Caplan, D. (1979). Neurolinguistics must be computational. *Behavioral and Brain Sciences*, *2*, 449–483.

Arbib, M. A., Conklin, E. J., & Hill, J. C. (1987). *From schema theory to language*. New York: Oxford University Press, pp. x + 253.

Arbib, M. A., Fagg, A. H., & Grafton, S. T. (2003). Synthetic PET imaging for grasping: from primate neurophysiology to human behavior. In F. T. Sommer, & A. Wichert (Eds.), *Exploratory analysis and data modeling in functional neuroimaging* (pp. 232–250). Cambridge MA: The MIT Press.

Arbib, M. A., & Lee, J. Y. (2007). Vision and action in the language-ready brain: from mirror neurons to semrep. In F Mele (Ed.), *LNCS*: *vol. 4729*. *Brain vision & artificial intelligence, 2007*, BVAI 2007, (pp. 104–123). Berlin, Heidelberg: Springer-Verlag.

Arbib, M. A., & Lee, J. Y. (2008). Describing visual scenes: towards a neurolinguistics based on construction grammar. *Brain Research*, *1225*, 146–162.

Auzias, G., Colliot, O., Glaunes, J. A., Perrot, M., Mangin, J. F., et al. (2011). Diffeomorphic brain registration under exhaustive sulcal constraints. *IEEE Transactions on Medical Imaging*, *30*, 1214–1227.

Bäß, P., Jacobsen, T., & Schröger, E. (2008). Suppression of the auditory N1 event-related potential component with unpredictable self-initiated tones: evidence for internal forward models with dynamic stimulation. *International Journal of Psychophysiology*, *70*, 137–143.

Binder, J. R., Frost, J. A., Hammeke, T. A., Bellgowan, P. S. F., Springer, J. A., et al. (2000). Human temporal lobe activation by speech and nonspeech sounds. *Cerebral Cortex*, *10*, 512–528.

Bishop, G. H., & Smith, J. M. (1964). The size of nerve fibers supplying cerebral cortex. *Experimental Neurology*, *9*, 483–501.

Bohland, J. W., Bullock, D., & Guenther, F. H. (2009). Neural representations and mechanisms for the performance of simple speech sequences. *Journal of Cognitive Neuroscience*, *22*, 1504–1529.

Bohland, J., Bullock, D., & Guenther, F. (2010). Neural representations and mechanisms for the performance of simple speech sequences. *Journal of Cognitive Neuroscience*, *22*, 1504–1529.

Bojak, I., Oostendorp, T., Reid, A., & Kötter, R. (2010). Connecting mean field models of neural activity to EEG and fMRI Data. *Brain Topography*, *23*, 139-49.

Chang, F. (2002). Symbolically speaking: a connectionist model of sentence production. *Cognitive Science*, *26*, 609–651.

Chang, F., Dell, G. S., & Bock, K. (2006). Becoming syntactic. *Psychological Review*, *113*, 234–272.

Dale, A. M., Fischl, B., & Sereno, M. I. (1999). Cortical surface-based analysis. I. segmentation and surface reconstruction. *NeuroImage*, *9*, 179–194.

David, O., & Friston, K. J. (2003). A neural mass model for MEG/EEG:: coupling and neuronal dynamics. *NeuroImage*, *20*, 1743–1755.

David, O., Harrison, L., & Friston, K. J. (2005). Modelling event-related responses in the brain. *NeuroImage*, *25*, 756–770.

David, O., Kiebel, S. J., Harrison, L. M., Mattout, J., Kilner, J. M., & Friston, K. J. (2006). Dynamic causal modeling of evoked responses in EEG and MEG. *NeuroImage*, *30*, 1255–1272.

David, O., Maess, B., Eckstein, K., & Friederici, A. D. (2011). Dynamic causal modeling of subcortical connectivity of language. *The Journal of Neuroscience*, *31*, 2712–2717.

Deacon, T. (2004). Monkey homologues of language areas: computing the ambiguities. *Trends in Cognitive Sciences*, *8*, 288–290. discussion 90-91.

Deco, G., Jirsa, V. K., Robinson, P. A., Breakspear, M., & Friston, K. (2008). The dynamic brain: from spiking neurons to neural masses and cortical fields. *PLoS Computational Biology*, *4*, e1000092.

Deco, G., Rolls, E. T., & Horwitz, B. (2004). "What" and "where" in visual working memory: a computational neurodynamical perspective for integrating FMRI and single-neuron data. *Journal of Cognitive Neuroscience*, *16*, 683–701.

Dell, G. S., Schwartz, M. F., Martin, N., Saffran, E. M., & Gagnon, D. A. (1997). Lexical access in aphasic and nonaphasic speakers. *Psychological Review*, *104*, 801–838.

Desikan, R. S., Ségonne, F., Fischl, B., Quinn, B. T., Dickerson, B. C., et al. (2006). An automated labeling system for subdividing the human cerebral cortex on MRI scans into gyral based regions of interest. *NeuroImage*, *31*, 968–980.

Destrieux, C., Fischl, B., Dale, A., & Halgren, E. (2010). Automatic parcellation of human cortical gyri and sulci using standard anatomical nomenclature. *NeuroImage*, *53*, 1–15.

DeWitt, I., & Rauschecker, J. P. (2012). Phoneme and word recognition in the auditory ventral stream. *Proceedings of the National Academy of Sciences*, *109*, E505-E14-E05-E14.

Dominey, P. F., & Arbib, M. A. (1992). A cortico-subcortical model for generation of spatially accurate sequential saccades. *Cereb Cortex*, *2*, 153–175.

Dominey, P. F., Arbib, M. A., & Joseph, J-P. (1995). A model of corticostriatal plasticity for learning oculomotor associations and sequences. *Journal of Cognitive Neuroscience*, *7*, 311–336.

Dominey, P. F., Hoen, M., & Inui, T. (2006). A neurolinguistic model of grammatical construction processing. *Journal of Cognitive Neuroscience*, *18*, 2088–2107.

Dominey, P. F., Inui, T., & Hoen, M. (2009). Neural network processing of natural language: II. towards a unified model of corticostriatal function in learning sentence comprehension and non-linguistic sequencing. *Brain and language*, *109*, 80–92.

Erman, L. D., Hayes-Roth, F., Lesser, V. R., & Reddy, D. R. (1980). The HEARSAY-II speech understanding system: integrating knowledge to resolve uncertainty. *Computing Surveys*, *12*, 213–253.

Evans, A.C., Collins, D.L., Mills, S.R., Brown, E.D., Kelly, R.L., & Peters, T.M. (1993). 1813 -17, *vols. 3-13-17*, *3*.

Evans, A. C., Janke, A. L., Collins, D. L., & Baillet, S. (2012). Brain templates and atlases. *NeuroImage*, *62*, 911–922.

Fagg, A. H., & Arbib, M. A. (1992). A model of primate visual-motor conditional learning. *Adaptive Behavior*, *1*, 3–37.

Fischl, B., Rajendran, N., Busa, E., Augustinack, J., Hinds, O., et al. (2008). Cortical folding patterns and predicting cytoarchitecture. *Cerebral Cortex*, *18*, 1973–1980.

Fischl, B., Sereno, M. I., & Dale, A. M. (1999). Cortical surface-based analysis. II: inflation, flattening, and a surface-based coordinate system. *NeuroImage*, *9*, 195–207.

Fischl, B., Van Der Kouwe, A., Destrieux, C., Halgren, E., Ségonne, F., et al. (2004). Automatically parcellating the human cerebral cortex. *Cerebral Cortex*, *14*, 11–22.

Friederici, A. D. (2002). Towards a neural basis of auditory sentence processing. *Trends in Cognitive Sciences*, *6*, 78–84.

Friederici, A. D. (2009). Pathways to language: fiber tracts in the human brain. *Trends in Cognitive Sciences*, *13*, 175–181.

Friederici, A. D. (2011). The brain basis of language processing: from structure to function. *Physiological Reviews*, *91*, 1357–1392.

Friederici, A. D. (2012). The cortical language circuit: from auditory perception to sentence comprehension. *Trends in Cognitive Sciences*, *16*, 262–268.

Friederici, A. D., & Kotz, S. A. (2003). The brain basis of syntactic processes: functional imaging and lesion studies. *NeuroImage*, *20*(Suppl. 1), S8-S17-S8-S17.

Garagnani, M., Wennekers, T., & Pulvermüller, F. (2008). A neuroanatomically grounded Hebbian-learning model of attention-language interactions in the human brain. *The European Journal of Neuroscience*, *27*, 492–513.

Grafton, S. T., Fagg, A. H., & Arbib, M. A. (1998). Dorsal premotor cortex and conditional movement selection: a PET functional mapping study. *Journal of Neurophysiology*, *79*, 1092–1097.

Gramfort, A., Papadopoulo, To, Olivi, E., & Clerc, M. (2011). Forward field computation with OpenMEEG. *Computational Intelligence and Neuroscience*, *2011*, 923703-03.

Grech, R., Cassar, T., Muscat, J., Camilleri, K. P., Fabri, S. G., et al. (2008). Review on solving the inverse problem in EEG source analysis. *Journal of Neuro Engineering and Rehabilitation*, *5*, 25.

Hagoort, P. (2005). On Broca, brain, and binding: a new framework. *Trends in Cognitive Sciences*, *9*, 416–423.

Hahne, A., & Friederici, A. D. (1999). Electrophysiological evidence for two steps in syntactic analysis: early automatic and late controlled processes. *Journal of Cognitive Neuroscience*, *11*, 194–205.

Hahne, A., & Friederici, A. D. (2002). Differential task effects on semantic and syntactic processes as revealed by ERPs. *Cognitive Brain Research*, *13*, 339–356.

Hallez, H., Vanrumste, B., Grech, R., Muscat, J., Clercq, W. D., et al. (2007). Review on solving the forward problem in EEG source analysis. *Journal of NeuroEngineering and Rehabilitation*, *4*, 46.

Heeger, D. J., & Ress, D. (2002). What does fMRI tell us about neuronal activity? *Nature Reviews Neuroscience*, *3*, 142–151.

Helmholtz, H. L. F. (1853). Ueber einige Gesetze der Vertheilung elektrischer Ströme in körperlichen Leitern mit Anwendung aud die thierisch-elektrischen Versuche. *Annalen der Physik und der physikalischen Chemie*, *9*, 211–233.

Hickok, G. (2009). The functional neuroanatomy of language. *Physics of Life Reviews*, *6*, 121–143.

Hickok, G., & Poeppel, D. (2007). The cortical organization of speech processing. *Nature Reviews Neuroscience*, *8*, 393–402.

Husain, F. T., Tagamets, M. A., Fromm, S. J., Braun, A. R., & Horwitz, B. (2004). Relating neuronal dynamics for auditory object processing to neuroimaging activity: a computational modeling and an fMRI study. *Neuroimage*, *21*, 1701–1720.

Jansen, B., & Rit, V. (1995). Electroencephalogram and visual evoked potential generation in a mathematical model of coupled cortical columns. *Biological Cybernetics*, *73*, 357–366.

Jurcak, V., Tsuzuki, D., & Dan, I. (2007). 10/20, 10/10, and 10/5 systems revisited: Their validity as relative head-surface-based positioning systems. *NeuroImage*, *34*, 1600–1611.
Keller, S. S., Crow, T., Foundas, A., Amunts, K., & Roberts, N. (2009). Broca's area: nomenclature, anatomy, typology and asymmetry. *Brain and Language*, *109*, 29–48.
Keller, S. S., Highley, J. R., Garcia-Finana, M., Sluming, V., Rezaie, R., & Roberts, N. (2007). Sulcal variability, stereological measurement and asymmetry of Broca's area on MR images. *Journal of Anatomy*, *211*, 534–555.
Kempen, G., & Hoenkamp, E. (1987). An incremental procedural grammar for sentence formulation. *Cognitive Science*, *11*, 201–258.
Kuperberg, G. R., McGuire, P. K., Bullmore, E. T., Brammer, M. J., Rabe-Hesketh, S., et al. (2000). Common and distinct neural substrates for pragmatic, semantic, and syntactic processing of spoken sentences: an fMRI study. *Journal of Cognitive Neuroscience*, *12*, 321–341.
Kutas, M., & Federmeier, K. D. (2011). Thirty years and counting: finding meaning in the N400 component of the event-related brain potential (ERP). *Annual Review of Psychology*, *62*, 621–647.
Kutas, M., & Hillyard, S. A. (1980). Reading senseless sentences: brain potentials reflect semantic incongruity. *Science*, *207*, 203–205.
Lecours, A. R., & Lhermitte, F. (1969). Phonemic paraphasias: linguistic structures and tentative hypotheses. *Cortex: A Journal Devoted to the Study of the Nervous System and Behavior*, *5*, 193–228.
Lee, J., & Barrès, V. (2013). From visual scenes to language and back via template construction grammar. *Neuroinformatics*,.
Lee, J., & Barrès, V. From visual scenes to language and back via Template Construction Grammar. *Neuroinformatics* (in press).
Leonard, C. M., Puranik, C., Kuldau, J. M., & Lombardino, L. J. (1998). Normal variation in the frequency and location of human auditory cortex landmarks. Heschl's gyrus: where is it? *Cerebral Cortex*, *8*, 397–406.
Lesser, V. R., Fennel, R. D., Erman, L. D., & Reddy, D. R. (1975). Organization of the HEARSAY-II speech understanding system. *IEEE Transactions on Acoustics, Speech, and Signal Processing*, *23*.
Liley, D. T. J., Cadusch, P. J., & Dafilis, M. P. (2002). A spatially continuous mean field theory of electrocortical activity. *Network (Bristol, England)*, *13*, 67–113.
Lopes da Silva, F., & Van Rotterdam, A. (1987). Biophysical aspects of EEG and MEG generation. In E. Neidermeyer, & F. L. D. Silva (Eds.), *Electroencephalography: basic principles, clinical applications and related fields* (pp. 15–28). Baltimore: Urban & Schwarzenberg.
Luck, S. J. (2005). *An introduction to the event-related potential technique*. A Bradford Book.
Lyttelton, O., Boucher, M., Robbins, S., & Evans, A. (2007). An unbiased iterative group registration template for cortical surface analysis. *NeuroImage*, *34*, 1535–1544.
Maess, B., Herrmann, C. S., Hahne, A., Nakamura, A., & Friederici, A. D. (2006). Localizing the distributed language network responsible for the N400 measured by MEG during auditory sentence processing. *Brain Research*, *1096*, 163–172.
Mangin, J-F., Jouvent, E., & Cachia, A. (2010). In-vivo measurement of cortical morphology: means and meanings. *Current Opinion in Neurology*, *23*, 359–367.
Matsumoto, R., Nair, D. R., LaPresto, E., Najm, I., Bingaman, W., et al. (2004). Functional connectivity in the human language system: a cortico-cortical evoked potential study. *Brain*, *127*, 2316–2330.
Mazziotta, J. C., Toga, A. W., Evans, A., Fox, P., & Lancaster, J. (1995). A probabilistic atlas of the human brain: theory and rationale for its development: the international consortium for brain mapping (ICBM). *NeuroImage*, *2*, 89–101.
McCallum, W. C., & Curry, S. H. (1980). The form and distribution of auditory evoked potentials and CNVs when stimuli and responses are lateralized. *Progress in Brain Research*, *54*, 767–775.
Michel, C. M., Murray, M. M., Lantz, G., Gonzalez, S., Spinelli, L., & Grave de Peralta, R. (2004). EEG source imaging. *Clinical Neurophysiology*, *115*, 2195–2222.
Miltner, W., Braun, C., Johnson, R., Jr, Simpson, G. V., & Ruchkin, D. S. (1994). A test of brain electrical source analysis (BESA): a simulation study. *Electroencephalography and Clinical Neurophysiology*, *91*, 295–310.
Naatanen, R., & Picton, T. (1987). The N1 wave of the human electric and magnetic response to sound: a review and an analysis of the component structure. *Psychophysiology*, *24*, 375–425.
Newman, S. D., Lee, D., & Ratliff, K. L. (2009). Off-line sentence processing: What is involved in answering a comprehension probe? *Human Brain Mapping*, *30*, 2499–2511.
Niedermeyer, E., & Silva, F. L. D. (2010). *Niedermeyer's electroencephalography: basic principles, clinical applications, and related fields*. Lippincott Williams & Wilkins.
Nunez, P. L., & Silberstein, R. B. (2000). On the relationship of synaptic activity to macroscopic measurements: does co-registration of EEG with fMRI make sense? *Brain Topography*, *13*, 79–96.
Nunez, P. L., & Srinivasan, R. (2005). *Electric fields of the brain: the neurophysics of EEG* (2nd ed.). USA: Oxford University Press.
Oostendorp, T. F., Delbeke, J., & Stegeman, D. F. (2000). The conductivity of the human skull: results of in vivo and in vitro measurements. *IEEE Transactions on Biomedical Engineering*, *47*, 1487–1492.
Oostenveld, R., Fries, P., Maris, E., & Schoffelen, J-M. (2011). FieldTrip: open source software for advanced analysis of MEG, EEG, and invasive electrophysiological data. *Computational Intelligence and Neuroscience*, *2011*, 1–9.
Osterhout, L., & Holcomb, P. J. (1992). Event-related brain potentials elicited by syntactic anomaly. *Journal of Memory and Language*, *31*, 785–806.
Pantev, C., Hoke, M., Lehnertz, K., Lütkenhöner, B., Anogianakis, G., & Wittkowski, W. (1988). Tonotopic organization of the human auditory cortex revealed by transient auditory evoked magnetic fields. *Electroencephalography and Clinical Neurophysiology*, *69*, 160–170.
Pascual-Marqui, R. D., Michel, C. M., & Lehmann, D. (1994). Low resolution electromagnetic tomography: a new method for localizing electrical activity in the brain. *International Journal of Psychophysiology: Official Journal of the International Organization of Psychophysiology*, *18*, 49–65.
Penke, M., Weyerts, H., Gross, M., Zander, E., Münte, T. F., & Clahsen, H. (1997). How the brain processes complex words: an event-related potential study of German verb inflections. *Cognitive Brain Research*, *6*, 37–52.
Phillips, C., Rugg, M. D., & Friston, K. J. (2002). Systematic regularization of linear inverse solutions of the EEG source localization problem. *NeuroImage*, *17*, 287–301.
Raettig, T., Kotz, S.A., Anwander, A., Friederici, A.D., & von Cramon, Yves D. (2007). Society for Neuroscience, San Diego, CA, U. S. A. Poster presented at Neuroscience Conference 2007.
Ritter, W., Vaughan, H. G., Jr, & Simson, R. (1983). 6 on relating event-related potential components to stages of information processing. In W. K. G. Anthony, & R. Walter (Eds.), *Tutorials in event related potential research: endogenous Components* (pp. 143–158). North-Holland.
Rupp, A., Uppenkamp, S., Gutschalk, A., Beucker, R., Patterson, R. D., et al. (2002). The representation of peripheral neural activity in the middle-latency evoked field of primary auditory cortex in humans. *Hearing Research*, *174*, 19–31.
Sarvas, J. (1987). Basic mathematical and electromagnetic concepts of the biomagnetic inverse problem. *Physics in Medicine and Biology*, *32*, 11–22.
Scherg, M., Vajsar, J., & Picton, T. W. (1989). A source analysis of the late human auditory evoked potentials. *Journal of Cognitive Neuroscience*, *1*, 336–355.
Schweighofer, N., Arbib, M., & Dominey, P. (1996). A model of the cerebellum in adaptive control of saccadic gain. *Biological Cybernetics*, *75*, 19–28.
Sotero, R. C., Trujillo-Barreto, N. J., Iturria-Medina, Y., Carbonell, F., & Jimenez, J. C. (2007). Realistically coupled neural mass models can generate EEG rhythms. *Neural Computation*, *19*, 478–512.
Stephan, K. E., Kamper, L., Bozkurt, A., Burns, G. A. P. C., Young, M. P., & Kotter, R. (2001). Advanced database methodology for the collation of connectivity data on the Macaque brain (CoCoMac). *Philosophical Transactions of the Royal Society B: Biological Sciences*, *356*, 1159–1186.
Tadel, Fo, Baillet, S., Mosher, J. C., Pantazis, D., & Leahy, R. M. (2011). Brainstorm: a user-friendly application for MEG/EEG analysis. *Computational Intelligence and Neuroscience*, *2011*.
Tagamets, M. A., & Horwitz, B. (1998). Integrating electrophysiological and anatomical experimental data to create a large-scale model that simulates a delayed match-to-sample human brain imaging study. *Cereb Cortex*, *8*, 310–320.
Tagamets, M. A., & Horwitz, B. (2000). A model of working memory: bridging the gap between electrophysiology and human brain imaging. *Neural Networks*, *13*, 941–952.
Upadhyay, J., Silver, A., Knaus, T. A., Lindgren, K. A., Ducros, M., et al. (2008). Effective and structural connectivity in the human auditory cortex. *The Journal of Neuroscience*, *28*, 3341–3349.
Van Essen, D. C. (2005). A population-average, landmark- and surface-based (PALS) atlas of human cerebral cortex. *NeuroImage*, *28*, 635–662.
Vigneau, M., Beaucousin, V., Hervé, P. Y., Duffau, H., Crivello, F., et al. (2006). Meta-analyzing left hemisphere language areas: phonology, semantics, and sentence processing. *NeuroImage*, *30*, 1414–1432.
Wahl, M., Marzinzik, F., Friederici, A. D., Hahne, A., Kupsch, A., et al. (2008). The human thalamus processes syntactic and semantic language violations. *Neuron*, *59*, 695–707.
Waxman, S. G., & Swadlow, H. A. (1977). The conduction properties of axons in central white matter. *Progress in Neurobiology*, *8*, 297–324.
Weiller, C., Bormann, T., Saur, D., Musso, M., & Rijntjes, M. (2011). How the ventral pathway got lost — and what its recovery might mean. *Brain and Language*, *118*, 29–39.
Wendel, K., Väisänen, O., Malmivuo, J., Gencer, N. G., Vanrumste, B., et al. (2009). EEG/MEG source imaging: methods, challenges, and open issues. *Computational Intelligence and Neuroscience*, *2009*.
Whitaker, H. A., & Selnes, O. A. (1976). Anatomic variations in the cortex: individual differences and the problem of the localization of language functions. *Annals of the New York Academy of Sciences*, *280*, 844–854.
Yvert, G., Perrone-Bertolotti, M., Baciu, M., & David, O. (2012). Dynamic causal modeling of spatiotemporal integration of phonological and semantic processes: an electroencephalographic study. *The Journal of Neuroscience*, *32*, 4297–4306.